Seasonal dynamics of chromophoric dissolved organic matter in Lake Kinneret: An investigation of fluorescent component changes in relation to microbial and phytoplankton productivity.

Research Thesis

In Partial Fulfillment of The
Requirements for the Degree of
Master of Science in Agricultural Engineering Sciences

Jonathan Liberzon

Submitted to the Senate of
the Technion - Israel Institute of Technology

Shvat, 5772 Haifa January 2011

Acknowledgements

Many thanks are due to Drs. Arkadi Parparov and Thomas Berman at the Kinneret Limnological Laboratory for their material and professional support, and to Prof. Tamar Zohary and Prof. Yossi Yacobi for graciously granting access to phytoplankton biomass and chlorophyll data. Thanks to Prof. Mikhail Borisover for his helpful suggestions during the planning phase of this research. My heartfelt thanks to the friendly and professional crew of the Hermona and Lillian research vessels, especially to Moty Diamond and Meir Arieli . My gratitude to Prof. Yoav Livni at the Technion Institute for the use of his spectrofluorometer. This research thesis was done under the supervision of Prof. Yohay Carmel in the Faculty of Agricultural Engineering at the Technion Institute, and Dr. Dror Angel in the Department of Marine Civilizations at Haifa University. I am extremely grateful for all of their help and encouragement. The generous financial help of the Faculty of Civil and Environmental Engineering at the Technion Institute is gratefully acknowledged.

Table of Contents

List of Figures:

Abstract

Energy and biomass flow through aquatic food webs as a result of photosynthesis, grazing and predation, and also through microbial consumption of detritus and dissolved organic matter (DOM). In some systems, such as Lake Kinneret, Israel, the microbial loop can represent the majority input into the heterotrophic food web, and yet the specific pathways of organic matter cycling within the water column remain poorly understood. Specifically, the interactions of chromophoric DOM and the microbial community have been difficult to characterize. Chromophoric (colored) dissolved organic matter (CDOM) is a complex mixture of amino acids, proteins, humic acids and sugars which absorb light. CDOM affects a number of ecosystem properties, including light availability, biological oxygen demand, micronutrient and reactive oxygen concentrations. Its chemical composition, and subsequently its specific optical absorbance and reactivity, is dependent on its source, which may be terrestrial (soil leachates) or biological. Biological production in the water column (algal, animal and microbial metabolic byproducts) takes the form of proteins and "marine" humic acids. Photoreactive processes break down CDOM into compounds of lesser molecular weights, either increasing or decreasing its lability as a microbial substrate. Due to its compositional variability, the controlling factors for CDOM lability remain poorly characterized. Still, researchers have developed new tools for quantifying and characterizing CDOM in natural systems, the most recent of which is spectrofluorometric analysis of the fluorescent fraction of CDOM. This method is able to separate and quantify the fluorescence of individual fractions of the total CDOM pool according to their optical excitation/emission peaks. The present study uses spectrofluorometry to investigate seasonal trends in CDOM fluorescence in Lake Kinneret, and attempts to relate the dynamics of CDOM fluorescence to microbial processing of algal-produced biomass within the lake. The study tracked three principal fluorescent components of the total fluorescent organic matter (FOM) pool in the upper mixed layer. In-situ timecourses showed that surface FOM was characterized by highly dynamic (max. Δ = 14%/week) protein-like fluorescence (p-comp: Excitation/Emission 280/322-382) and weaker, relatively stable 'terrestrial' and 'marine' humic-like components (t-comp: 360/458 and m-comp: 310/394) during the winter production period. T-comp and m-comp were linearly related from turnover until late summer. All three components showed gradual reductions after lake stratification. P-comp was linearly related to phytoplankton biomass, chlorophyll a and secchi depth in situ. Subsequent dark incubations of water sampled at naturalistic DOM concentrations in situ revealed p-comp and m-comp production, with up to 91% (m-comp) and 73% (p-comp) of integrated FOM production and up to 52% of

integrated microbial carbon production originating from the particulate fraction. T-comp concentrations did not significantly change in incubation. Seasonal increases in phytoplankton productivity and microbial production were reflected by increased FOM production in incubation. This study supports the relationship between microbial processing of algal biomass and the production of protein-like and marine humic-like FOM. The lack of m-comp accumulation in surface waters, despite m-comp production in incubation, supports the role of rapid photobleaching in the regulation of this component. The ability of p-comp to trace seasonal algal dynamics is demonstrated, though this relationship was highly dependent on the temporal resolution of sampling.

List of Abbreviations

OM: Organic Matter

CDOM: Chromophoric Dissolved Organic Matter

FOM: Fluorescing Organic Matter

DOM: Dissolved Organic Matter

POM: Particulate Organic Matter

TOM_L/POM_L/DOM_L: Total/Particulate/Dissolved labile organic matter

DOC/POC: Dissolved/Particulate organic carbon

DIC: Dissolved inorganic carbon

P-comp: Protein-like fluorescent component

M-comp: Marine humic-like fluorescent component

T-comp: Terrestrial humic-like fluorescent component

ChlA: Chlorophyll a

Sig: Statistically significant ($p<0.05$)

Ex: Fluorescent excitation wavelength

Em: Fluorescent emission wavelength

FU: raw fluorescent units (machine counts)

AUC: Area under the curve

BOD: Biological Oxygen Demand

LMW/HMW: Low Molecular Weight/ High Molecular Weight

Introduction

Aquatic ecosystems, like terrestrial ecosystems, cycle compounds through abiotic and biotic forms. During photosynthesis, photoautotrophs use the sun's energy to convert inorganic compounds (mainly oxygen-bound forms of carbon, hydrogen, nitrogen and phosphorus) into organic matter (OM), which forms the basis of the aquatic food web. Organic matter in the form of algae and other autotrophs is subsequently consumed by higher-order heterotrophs. Secondary, tertiary and higher-level cycling of OM is accomplished by predation. At each level of this "living" food web, some OM is also diverted into the detrital trophic pathway and the microbial loop in the form of dead organisms, senescent cells, metabolic wastes (e.g. feces) and exudates. These forms of OM are functionally defined as particulate or dissolved organic matter (POM or DOM) depending on their size, and are continuously released by organisms into the water column. DOM and POM are removed from aquatic systems through consumption, sedimentation, and physical transport such that their concentrations are controlled by a combination of biotic and abiotic processes (Fig. 1). Production and removal processes, whose rates vary seasonally, function simultaneously to maintain dynamic seasonal DOM and POM concentrations within aquatic systems (For a review of carbon cycling in aquatic systems, see Barnes & Mann 1991).

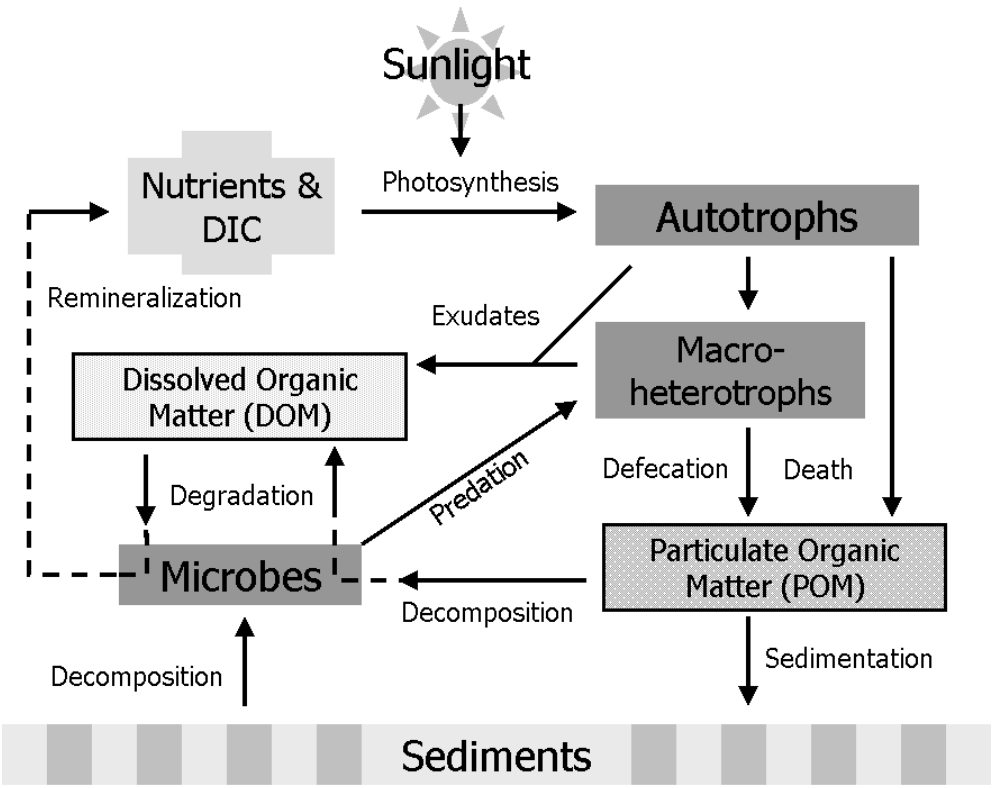

Figure 1: Schematic representation of the role of dissolved organic matter (DOM) and particulate organic matter (POM) in aquatic ecosystems. "Nutrients" refer to inorganic nitrogen, phosphorus and micronutrients (e.g. iron). Dissolved inorganic carbon (DIC) includes bicarbonate and carbonate species.

Particulate organic matter dynamics

Particulate organic matter (POM), the organic component of the water column, is comprised of a number of non-living, autochthonous biological components such as feces, dead organisms, cells, tissues, and other elements of the detrital food web. In freshwater or coastal aquatic systems with runoff or riverine input, the majority of POM is generally allochthonous material such as leaf litter or the products of plant breakdown, humus particles, macrophyte remains, etc. In the deep ocean, the majority of POM is produced within the water column, and POM loading often tracks local primary production rates as autotrophic biomass dies or is consumed and excreted by zooplankton (Hansell & Carlson 2002). Even in deep water, atmospheric deposition is responsible for considerable inputs of terrigenous POM aerosols (Hernes & Benner 2006). POM, along with inorganic suspended solids, absorbs light entering aquatic environments and may dramatically alter the available light field. By absorbing light at wavelengths that match the absorption range of photosynthetic pigments, POM can contribute to limiting primary production, especially at depths where light overtakes nutrients as the limiting resource for photosynthesis. POM is physically removed from the water column as it sinks and is deposited in sediments, with sinking rates increasing as particle size increases. As POM particles sink, they are colonized by heterotrophic bacteria and utilized for microbial growth. Due to the high metabolic rate of attached bacteria, the majority of easily biologically degradable POM particles (specifically fecal pellets) are disintegrated in the upper 50-100m of the water column (at least in oceanic systems; LeFèvre et al. 1998), which means that much of the organic matter trapped in such particles is solubilized and released within the water column. Thus, microbial breakdown of POM produces DOM, which remains available to bacterial utilization, as well as inorganic nutrients and microbial biomass, which cycle back into the autotrophic and microbial loops. The remaining POM accumulates in bottom sediments, where further decomposition is achieved by sediment microbes and detritivores (see Pomeroy & Wiebe 1988, Pomeroy et al. 2007, and references therein for a review of the microbial loop and microbe-POM/DOM interactions).

Dissolved organic matter

Functionally defined, dissolved organic matter (DOM) includes all complex organic molecules smaller than 0.45 µm (Mopper & Degens 1979). DOM is added to aquatic systems in many forms, including exudates from phytoplankton, zooplankton and fish, soil

leachates, and byproducts of microbial breakdown of POM and benthic sediments. DOM constitutes one of the largest carbon reservoirs on earth (Mopper & Degens 1979); the reservoir of fixed carbon stored in oceanic DOM, for example, is roughly equivalent to the amount of carbon stored in the atmosphere as CO_2 (Ogawa et al. 2001). DOM also serves as an important energy and biomass conduit in aquatic systems. The aquatic DOM pool consists of a complex array of both bioavailable and refractory chemical compounds, including carbohydrates, amino acids, humic acids, lignin phenols (in ecosystems receiving terrestrial runoff) and a small concentration of lipids (Amon et al. 2001; Benner 2002; Hernes & Benner 2006). While DOM is constantly produced in aquatic systems, the majority of new DOM is quickly broken down into smaller, less complex molecules through microbial processing (Findlay & Sinsabaugh 2003). The fraction of DOM that is readily digestible by microbes, called the *labile* or bioavailable fraction, has been identified as primarily carbohydrates and amino acids (Ochiai et al. 1980), specifically neutral sugars and L amino acids (Weiss & Simon 1999, Amon et al. 2001). Microbial decomposers favor high molecular weight (HMW) DOM compounds as food sources, and this selective degradation leads to the accumulation of low molecular weight (LMW) *refractory* DOM , which persists in natural waters for long periods (up to thousands of years) without decomposing (Amon & Benner 1996, Ogawa et al. 2001). Unlike POM, dissolved organic matter does not settle out of aquatic ecosystems, and for this reason the majority of (accumulated) marine DOM is refractory and of low molecular weight (Amon & Benner 1996; Ogawa et al. 2001 and refs therein).

As the intermediary destination of exudates and decomposition products and a major source of growth substrates for the microbial community, the DOM pool is the major site of recycling and remineralization within aquatic ecosystems. Inorganic nutrients released during microbial breakdown of POM and DOM facilitate primary production during periods of nutrient limitation (Pomeroy et al. 2007), and the same process underlies the hypolimnetic buildup of nutrients that produces seasonal peaks in algal production following the breakdown of the thermocline, when these nutrients are mixed to the surface (Hart et al. 2000). DOM availability is the predominant regulator of microbial production (del Giorgio & Cole 1998), which in turn represents a large (sometimes majority) fraction of total OM production within aquatic systems (Pomeroy et al. 2007; Fenchel 2008; Berman et al. 2009). Understanding the flow of labile compounds through this aquatic pool is essential to understanding the mechanisms of carbon storage, recycling and sedimentation in fresh and marine waters.

In addition to microbial degradation, the chemical properties of DOM are also altered by exposure to sunlight. Moran & Zepp (1997) reviewed a number of studies in which irradiation of natural water samples increased bacterial production rates, suggesting that light increases the bioavailability of DOM. Recent studies (e.g. Benner & Biddanda 1998, Tranvik & Bertilsson 2001, Rosenstock et al. 2005, and others) have sought to gain a better understanding of the effect of irradiation on various forms of DOM, and have found the relationship between light exposure and bioavailability more complicated than previous studies had suggested. Apparently, photodegradation of aromatic rings by light in the UV range may either reduce or enhance the bioavailability of organic compounds as substrates for microbial growth, depending on their age and composition. In marine systems, Rosenstock et al. (2005) found that irradiation of seawater DOM with UV-B light either increased or decreased microbial metabolism of glucose, depending on the water source and available concentration of humic-bound dissolved amino acids. Benner & Biddanda (1998) found variable (and opposite) effects of sunlight exposure on bacterial production. Photoirradiation of samples prior to dark incubation reduced bacterial production in surface water, and boosted bacterial production in deep water. Tranvik & Bertilsson (2001) found that irradiation of terrestrial-source DOM increased bacterial production, while irradiation of autochthonous, algal-sourced DOM reduced it. Smith & Benner (2005) found similar production increases in irradiated terrestrial DOM, but these increases were accompanied by larger increases in bacterial respiration and demand for inorganic nutrients, ultimately reducing growth efficiency. Finally, Pérez & Sommaruga (2007) found that solar irradiation reduces bacterial productivity in lake water as well as terrestrial and phytoplankton derived DOM isolates. Thus, the effect of photodegradation on DOM is highly variable and requires additional study with respect to the interactive effect of DOM source, history and composition. In any case, photochemical degradation is extremely important on a global and local scale, since this may be the only process in which large fractions of biologically refractory DOM are recycled through aquatic systems, either through direct remineralization or subsequent microbial consumption (Morris & Hargreaves 1997). Mopper et al. (1991) suggest that photodegradation may, in fact, be the limiting step in the recycling of a large fraction of oceanic DOM.

Chromophoric DOM

While our understanding of the complex effect of photoirradiation on DOM bioavailability may be relatively recent, the importance of light absorption by DOM in aquatic systems

has been the focus of research for decades. Early researchers identified gelbstuff or "yellow substance" as an important light-limiting factor in natural waters, especially those influenced by significant runoff from soils (Siegel et al. 2002). Later renamed chromophoric dissolved organic matter (CDOM), this is the optically active fraction of the DOM pool which absorbs light in the 200-500 nm range. CDOM has been described as a fast-cycling pool of DOM with additional ecologically important properties such as the absorption of ultraviolet and photosynthetically active radiation (PAR) (Ferrari & Tassan 1991, Miller 1999). As light in the 400-500 nm bandwidth is absorbed by CDOM within the water column, the vertical penetration of PAR is diminished, thereby limiting the depth of the photic zone and subsequently reducing overall primary production. At the same time, attenuation of UV light protects organisms in shallow waters from DNA damage, and CDOM is the dominant regulator of UV penetration in the open ocean (Tedetti & Sempere 2006). As described above for DOM, CDOM is photoreactive, degrading to an array of compounds with varying levels of bioavailability, including labile bacterial substrates and inorganic nutrients. Research into CDOM photochemistry has also identified novel degradation products such as reactive oxygen species and compounds with high affinities for micronutrient metals, especially iron species (Blough & Del Vecchio 2002). Reactive oxygen species produced during CDOM degradation (such as hydrogen peroxide, superoxide, hydroxyl, etc.) damage DNA and other cellular components, increasing the physiological stress of unicellular organisms within the water column. Removal of soluble micronutrient ions through complexation with CDOM and subsequent sedimentation may limit primary production in high-nutrient-low-productivity regions, which characterize large swaths of the world oceans. Primary production in offshore regions of the Mediterranean, for example, is primarily limited by concentrations of bioavailable iron (Pitta et al. 2005). Thus, CDOM degradation, accomplished by microbial and photochemical processes can both support and inhibit algal and bacterial production in aquatic systems. Moreover, the global CDOM carbon pool is so large that changes in its dynamics could profoundly affect global carbon cycling and atmospheric carbon concentrations. Understanding the ecological role of CDOM, including dynamics of production and degradation, is critical to our understanding of global carbon budgets, nutrient cycling and aquatic trophic structures.

Spectrophotometric quantification of CDOM

Initially, quantification of CDOM was accomplished based on its relevant optical properties, specifically its light absorption profile. CDOM absorbs light most strongly at short wavelengths, resulting in an absorption spectrum which drops exponentially from about 300nm to negligible absorption around 550 nm. In order to establish a uniform index for measuring and reporting CDOM absorbance, researchers fit this spectrum to the function:

$$a(\lambda) = 2.303D(\lambda)/r$$

where

$a(\lambda)$ = the uncorrected CDOM absorption at wavelength λ
$D(\lambda)$ = the optical density at wavelength λ
r = the cuvette path length in m

and subsequently used the value of the absorption coefficient *a* to quantify CDOM in their work. This method had several drawbacks. First, in many oceanic and oligotrophic freshwater systems, the spectrophotometric absorption signal of CDOM was so weak that it was necessary to concentrate the CDOM in water samples in order to obtain a reliable optical signal. This restricted the number of samples that could be collected, especially due to long processing times, and introduced a significant risk of contamination during the concentration phase (Coble 1996). In highly turbid ecosystems, the opposite problem exists: light penetration may be so limited that dilution of samples with pure water is necessary to facilitate the passage of adequate quantities of light through the sample during spectrophotometry. Moreover, a sample's absorption at any one wavelength provides no useful information about its chemical composition (apart from a rough measure of aromaticity).

Fluorescent quantification of CDOM

In the last decade or so, researchers have adopted new optical methods for characterizing and quantifying CDOM based on fluorescence. Certain compounds within the dissolved organic matter pool contain fluorophores, molecules with functional groups that absorb light at one wavelength (the excitation wavelength), and emit a portion of this energy by releasing photons at another wavelength (the emission wavelength). In natural CDOM, fluorescence is primarily attributed to aromatic ring structures within proteins, humic and fulvic acids (Coble 1996), and was adopted as a more sensitive method of quantifying CDOM. Fluorescence testing requires active excitation using a light source, allowing for accurate, sensitive examination of small volumes at naturalistic concentrations. Several

studies have found robust linear (Ferrari & Tassan 1991; Hoge et al. 1993; Ferrari et al. 1996; Vodacek et al. 1997; Ferrari & Dowell 1998; Ferrari 2000; Kowalczuk et al. 2003) or non-linear (Zhao et al. 2009) relationships between CDOM absorbance and fluorescence, which may vary as a function of productivity and ecosystem type, suggesting that fluorescence can serve as a good indicator of CDOM dynamics. Initially, CDOM fluorescence was quantified at arbitrarily selected wavelengths, until two distinct fluorescence peaks were related to dissolved humic acids and amino acids in seawater. Since the shape of these peaks was somewhat variable, researchers began to use fluorescence contouring (the measurement of emission spectra at a range of consecutive excitation wavelengths) to produce excitation-emission matrices (EEMs) for water samples. These matrices provide a more detailed picture of the fluorescence "signature" of a water sample by capturing all the fluorescence responses of the sample while also tracking shifts in the position or shape of known fluorophore peaks. Coble (1996) was the first to use fluorescence excitation/emission matrices to track specific fluorophores in natural waters, allowing researchers to identify, quantify and assess the bioavailability of fluorescing DOM originating from distinct sources.

Primary fluorescent components of FOM

Three primary classes of fluorescent organic components have been characterized according to the location of their fluorescent emission peaks (Coble, 1996). Peaks centered around excitation/emission values of 220/303 and 275/345 represent protein-like components, specifically the fluorescent amino acids tyrosine and tryptophan. Two classes of peaks track aromatic humic acid fluorescence, one class representing humics of primarily terrestrial origin and one class representing humics produced within the water column, dubbed "marine" humics in early ocean-based studies (Donard et al. 1989; Coble et al. 1990; De Souza Sierra et al. 1994). Subsequent adoption of parallel factor analysis (PARAFAC) (Stedmon & Bro 2008) as a popular statistical tool for separating fluorescent components in a wide array of waters where emission peaks may overlap, has primarily reinforced the three original peak classes and approximate locations, while adding several more peaks that can be used to track anthropogenic pollutants (Stedmon et al. 2003, Cammack et al. 2004, Murphy et al. 2008, Borisover et al. 2009). PARAFAC uses a decompositional statistical model to quantify and locate the component peaks which combine to form a fluorescent signature. This tool has allowed researchers to standardize the identification of component peaks, and allowed for the isolation of overlapping or low-intensity peaks that would prove difficult to identify visually.

In-situ studies have found that these three classes of fluorescent organic matter (FOM) differ in their distribution and reactivity in natural waters. The terrestrial humic-like fluorescent organic matter component (t-comp) of the FOM pool has been used to track riverine or estuarine input into gulfs, bays and deltas (Coble 1996; Stedmon et al. 2003; Murphy et al. 2008; Kowalczuk et al. 2009), while the "marine" humic-like fluorescing component (m-comp) has been related to biological production within the water column (Stedmon et al. 2003; Chen et al. 2004; Nieto-Cid et al. 2006; Murphy et al. 2008). In some studies, these two components have been found to co-vary (Stedmon & Markager 2005b), even behaving as one component in one freshwater lake system (Borisover et al. 2009) and changing independently in the open-ocean (Murphy et al. 2008). Protein-like fluorescing components (p-comp) have been shown to correlate with phytoplankton and bacterial production (Rochelle-Newall & Fisher 2002; Chen et al. 2004; Cammack et al. 2004; Stedmon & Markager 2005; Nieto-Cid et al. 2006; Hudson et al. 2008), though the relationship is not clear. One problem is that there have been few seasonal studies to track FOM component dynamics in-situ, especially in fresh water; researchers have instead focused on spatial studies and incubation experiments. To my knowledge, Borisover et al.'s (2009) study of Lake Kinneret remains the only study to track these three (protein-like, marine and terrestrial humic-like) fluorescent components year-round in a freshwater lake.

In general, a number of biological pathways have been proposed for FOM production, consumption and overall regulation, and these have been tested in controlled laboratory incubations and cultures. In-situ studies have found conflicting relationships between FOM/CDOM and phytoplankton productivity, with some studies reporting no consistent correlation between FOM and chlorophyll a (ChlA) (Chen et al. 2004a, Borisover et al. 2009), while others suggest that a relationship may only be discernable during high-production algal blooms (Stedmon & Markager 2005a; Zhao et al. 2009). Blooms induced in nutrient amended laboratory algal cultures (Rochelle-Newall & Fisher 2002) did not show FOM enhancement related to increases in ChlA or phytoplankton biomass. On the contrary, these studies suggest that microbial decomposition of phytoplankton-produced DOM is the factor that determined FOM concentration. This hypothesis is bolstered by several studies that investigated the relationship between CDOM and microbial activity. In nutrient-amended seawater incubations, CDOM absorbance was correlated with rising microbial cell densities (Nelson et al. 2004), and p-comp has been shown to accurately track the fraction of microbially bioavailable DOM in fresh water, as measured by biological oxygen demand (Hudson et al. 2008). Cammack et al. (2004) found that p-comp

accounted for 44-55% of in-situ variability in bacterial production, respiration and carbon consumption, as well as total phytoplankton respiration in a series of lakes. A number of incubation studies have suggested that p-comp and m-comp are both produced and consumed by oceanic microbes, and that individual components only accumulate when high concentrations of DOM from phytoplankton or zooplankton sources are available (Nelson et al. 2004; Nieto-Cid et al. 2006). Stedmon & Markager (2005a) found that p-comp co-varied seasonally with t-comp in one estuarine system and suggested that decomposition of terrestrial DOM may also contribute to p-comp accumulation.

DOM dynamics in Lake Kinneret

Lake Kinneret, Israel, is a warm mesotrophic lake with majority water inputs in winter and negligible inputs in summer. The lake has a history of dramatic spring algal blooms and strong summer stratification. The lake serves as an essential source of drinking water for the state of Israel, with an average of 550 million cubic meters pumped out annually to supply the National Water Carrier and nearby consumers (Markel 2008). Yearly carbon input to the lake is dominated by an early springtime algal bloom which is quickly processed by the microbial community (Hart et al. 2000). In one study, labile organic matter loads, as measured by 30 day BOD, were as much as 900% higher during the spring bloom when compared to the yearly minimum (Ostapenia et al. 2009). A number of studies have demonstrated the importance of the microbial loop in processing gross primary production in this lake, as evinced by strong correlations between bacterial and primary production (Berman et al. 2001), and a bacterial carbon demand (production + respiration) at levels approaching or exceeding gross primary production (Berman et al. 2009). Hart et al. (2000) found that bacterial production tracked detrital carbon loading proportionally, and cite unpublished work by Berman showing that Kinneret bacterial communities are primarily carbon limited. In short, the great majority of Kinneret carbon input is from phytoplankton production, which passes through the particulate and dissolved organic carbon reservoir and is processed by bacteria.

Historically, the stable spring bloom in Lake Kinneret was overwhelmingly dominated by the dinoflagellate *Peridinium gatunase.* Total plankton biomass rose in winter, peaked in spring with the *Peridinium* bloom, and declined in early summer to a low baseline maintained until the onset of mixing (Pollingher 1981). Since 1994, however, this pattern has been disrupted. Recent years have seen a reduction in *Peridinium* and an increase in

diatoms, chlorophytes, and cyanobacteria, including nitrogen-fixing species. Blooms are less predictable, with some years characterized by smaller and more frequent bloom events, though peaks in algal biomass still occur mostly between February and May (Zohary 2004). The spring algal blooms follow the epilimnetic nutrient input of the winter turnover, and usually begin concurrently with, or shortly after, the year's primary runoff input in Jan/Feb. The seasonal separation of runoff input and production peaks, concentrated input and bacterial processing of phytoplankton DOM/POM in early spring, and large fraction of carbon respired by microbes (40% on average; Hart et al. 2000), all make Lake Kinneret an excellent model ecosystem for isolating FOM production and measuring changes at short timescales and natural concentrations.

Within the photic zone, the standing organic carbon pool is roughly 75% dissolved organic carbon (DOC) and 25% particulate organic carbon (POC), the labile fraction representing about 12% of total DOC and 9% of total organic carbon (TOC) (Berman et al. 2004). This distribution reflects the general trend for rapid processing of labile DOM and subsequent buildup of refractory organic compounds. A 30 day BOD study by Parparov (pers. communication) suggests that up to 70% of POC in the Kinneret is biologically labile given adequate processing time, though turnover rates for the most labile fraction of both DOC and POC are around 4 days (Berman et al. 2004). An earlier study of FOM in Lake Kinneret and its catchment basin by Borisover et al. (2009) identified three major FOM components using PARAFAC statistical analysis. The greatest fluorescence contribution in the Kinneret was from a protein-like component (p-comp), characterized by a consistent surface distribution and a decrease in concentration with depth. A marine (m-comp) and terrestrial (t-comp) humic-like component were also found. These correlated weakly in the Kinneret, though they were tightly coupled in the upstream waters of the Jordan river. During stratification, buildup of t-comp was identified near benthic sediments, though overall, the best predictor of increasing fluorescent humic compounds was the distance from the surface, suggesting that photoreactive processes play an important role in mediating concentrations of these components.

This study tracked FOM, phytoplankton and microbial productivity during the winter-spring production period in Lake Kinneret (Israel) to further clarify the role of phytoplankton and microbial production in controlling *in situ* FOM concentration and composition. Data were collected at higher temporal resolutions than previously reported in situ, and incubations were performed using unamended lake water at natural concentrations of FOM, DOM and phytoplankton biomass.

Working hypotheses

Based on the work of Rochelle-Newall & Fisher (2002), Cammack et al. (2004), Hudson et al. (2008) and Borisover et al. (2009), I hypothesized that microbial degradation of algal POM/DOM controls protein-like and marine humic-like FOM concentrations within the lake. Protein-like CDOM fluorescence was predicted to track algal production peaks, with a delayed fluorescence signal reflecting microbial degradation of dead algal biomass. This initial p-comp signal was predicted to decline in summer as protein-like FOM is processed by the microbial community, producing an increase in marine humic-like FOM and non-fluorescing DOM. Terrestrial humic-like FOM was predicted to track riverine input from the Jordan river during the brief period of heavy runoff in winter. Dissolved organic matter (including the dissolved fraction of FOM) was expected to serve as the primary labile growth substrate for bacteria, and the primary source of new FOM produced in incubation.

Objectives of this study

1. To characterize the dynamics of three major CDOM components (p-comp, m-comp, t-comp) during the winter production period at a greater temporal resolution than has been previously reported for Lake Kinneret.
2. Examine the relationships between CDOM, microbial activity and seasonal algal production.
3. Use lake water incubations to track the fate of natural lake POM and DOM during microbial degradation.
4. Determine the composition of microbially digested CDOM, and whether dissolved or suspended substrates are more critical production sources.

Methods

Study site

Samples were collected from 'Station A' (32'49.350" N x 35'35.487" E), an established data gathering point of the Kinneret Limnological Laboratory (KLL, IOLR) monitoring program. The site is located at one of the deepest points in the lake (mean yearly depth c. 39 m), where seiche influence on thermocline depth is minimal and horizontal mixing is maximal (Fig. 2). Surface water at this location was assumed to be laterally well-mixed and accurately represent an average of overall lake characteristics in the upper mixed layer. In other words, due to constant mixing, we assumed that concentrations of DOM, POM, FOM, microbes, chlorophyll and phytoplankton at Station A were essentially equivalent to the average concentrations of these measures sampled at equivalent depths throughout the lake. This assumption is supported by Gafny & Gasith (1993), who concluded that, among all monitoring locations, Station A data are the most representative of conditions throughout the lake, apart from the littoral (lake shoreline).

Figure 2: Samples were gathered at Station A, located centrally in Lake Kinneret, Israel

Timecourse sampling

Sampling began in early January 2009, shortly after the breakdown of the thermocline and initiation of total mixing (c. 15/1/09). An 8 month (January-August) sampling period was

selected to capture seasonal changes, including: the anticipated high-volume runoff events of January-March, the high productivity of early spring (February-April), and the post-stratification period (May-July). Thermal stratification in Lake Kinneret is followed by reduced epilimnetic productivity, nutrient limitation and increased microbial activity in summer (Berman & Pollingher 1974; Hart et al. 2000). Samples were collected more frequently during the dynamic winter-spring production period (Fig. 3) to capture the effect of changes in lake productivity on the OM pool and on FOM. Sampling continued through a well-mixed winter period and well-past stratification, which began in April. Summer lake conditions were characterized by an anoxic hypolimnion below aprox. 15 m depth, and a well-mixed epilimnion. Throughout the study, the photic zone, as determined by Secchi depth, ranged from approx. 2.0-4.5 m in depth.

Station A was accessed aboard the motorized KLL research vessels Lillian and Hermona and by tying up to a fixed-chain buoy marking the station. Each day on which samples were taken from the lake represents an individual *timepoint*. Lakewater samples were drawn from a depth of 1m using a hand-winched 5L PVC water sampler (Hydro-Bio). A sampling depth of 1m was selected in order to capture near-surface water while avoiding highly concentrated algal/cyanobacterial colonies which may form at the air-water interface. Surface water was selected since intensive wind-driven mixing produces a uniform upper mixed layer in the Kinneret which is mixed on timescales of several hours (Yacobi, personal communication). Bacterial production, the hypothesized driver of conservative FOM change in this study, did not vary considerably throughout Lake Kinneret's epilimnion from 2000-2007 (Berman et al. 2010). Therefore, near-surface samples are a representative measure of overall epilimnetic FOM in this water body, since the entire epilimnion is well-mixed vertically. Timepoints were sampled in triplicate, with a separate cast for each of the three sample bottles per timepoint. This multi-cast method was chosen in order to capture any small-scale horizontal spatial variations within the water column and to avoid psuedoreplication. Secchi disk depth casts (Tyler 1968) were performed immediately after sampling to track changes in water clarity within the photic zone. Casts were performed between 8AM and 10AM on the shady side of the vessel, without sunglasses, using a standard 20 cm secchi disk.

Samples for FOM and bacterial production measurement were transported to the laboratory in brown-tinted, 130mL glass bottles, which had been acid-washed and rinsed with HPLC grade H_2O (Sigma) to remove traces of organic matter. Light exposure of samples was avoided in order to prevent post-sampling photosynthesis or photochemical alteration of

dissolved organic matter. Samples were kept on ice in darkness until fluorescence testing, which occurred within 7 hours of sampling unless otherwise noted. Cold transport was chosen to reduce cellular metabolism, minimizing microbial degradation/production of OM and algal exudation.

To examine the relationship between algal production and FOM in the lake, fluorescence timecourse data were tested for correlation with phytoplankton biomass and chlorophyll a data from the same sampling day or within two days of sampling. To examine the effect of external sources on Kinneret FOM, Jordan river flow volume data (provided by the Israel Water Authority) and lake level data (provided by the Kinneret Limnological Laboratory) were obtained and compared to this study's seasonal FOM timecourse. While the Jordan river is not the only source of water input to the lake, it represents the major input by volume. Furthermore, runoff input is directly dependent on precipitation, and since river flow is driven by precipitation within the Kinneret watershed, it was assumed that Jordan River flow data track the total combined flows into the lake.

Bacterial production

Total bacterial production was chosen as a measure of DOM-altering activity within the microbial loop. Twice per month, two 1.9mL subsamples were taken from each of three replicate sampling bottles and inoculated with 10uL ^{3}H radiolabelled leucine (Amersham Biosciences corp) for bacterial productivity assays (Simon & Azam 1989). One triplicate series was killed and proteins precipitated with 100uL of 100% trichloroacetic acid (TCA) solution (Sigma). Live and killed leucine-amended samples were incubated in the dark at room temperature (20°C) for 4-16 hours, after which TCA was added to the remaining samples. Samples were stored an additional 24-72 hours at room temperature (20°C) before analysis, based on the previous experience that triplicate scintillation counts were more precise (more tightly clustered) after 24 hours (Berman, personal communication). Prior to radioactivity counting, samples were centrifuged for 10 minutes at 14000 RPM to settle out cells and the supernatant was decanted to eliminate unbound tritiated leucine. Pellets were washed with 1mL of 5% TCA solution, centrifuged, decanted, and 1mL scintillation fluid (Perkin Elmer Ultima Gold) was added to pellets. Samples were counted in a Packard Tri-Carb 2100TR liquid scintillation counter. Incorporated leucine was calculated by comparing the radioactivity of samples killed pre and post incubation, and this value was converted to daily carbon production (Simon & Azam 1989).

Fluorescence determination

Initially, in order to control for the fluorescence of POM (specifically living algal cells), this study intended to track only the dissolved fraction of the FOM pool in-situ. Separation of the dissolved from the suspended fraction involved filtration using precombusted (550° C, 3 h) Whatman GF/F glass-fiber filters. Early on in the study, significant logistical time constraints (resulting from lengthy shipboard and overland transportation times) were identified, which made filtration of every in-situ sample unfeasible. In the only previous study of FOM in the Kinneret, Borisover et al. (2009) used unfiltered lake water to build fluorescence excitation/emission matrices (EEMs) based on preliminary data showing that fluorescence peak intensities were not considerably different in filtered and unfiltered samples (Borisover, personal communication). Moreover, a recent study of labile DOM in Lake Kinneret and five other lakes found that the dissolved fraction dominated the total organic carbon pool at all six sites (Ostapenia et al. 2009), suggesting that this fraction may also dominate fluorescence signatures within the lake. To test whether the total fluorescing fraction could be used as an approximation for dissolved fluorescence in this study, a sample was collected in early January and split into two subsamples. One subsample was filtered to isolate the dissolved fraction, one remained unfiltered, and both were tested for fluorescence. Subsequent analysis revealed that there was no considerable difference between filtered and unfiltered samples with respect to this study's target fluorescent components (see results). Based on these findings, I decided to use only unfiltered samples for in-situ fluorescence determination in this study.

Fluorescence excitation/emission matrices were produced by reading the fluorescence of Kinneret water samples in a 3ml quartz cuvette on a Fluorolog 3-22 spectrofluorometer (Jobin Yvon, Horiba, Longjumeau cedex, France). This instrument uses a xenon lamp for excitation, and the fluorescence sensor was set at a 90° angle to the excitation source to reduce the amount of excitation light reaching the emission sensor. Excitation/emission matrices (EEMs) were produced by excitation at 270-350 nm and emission measurement at 290-462 nm with a band pass width of 5nm. To control for machine variation in excitation light intensity, emission signal values were divided by lamp intensity. HPLC grade H_2O (Sigma) was used as a comparative control for fluorescence and to track signal/noise ratio over the course of the study. The fluorescence signature of HPLC-grade water is monitored

by the manufacturer and is free of peaks within the range of interest of this study. See appendix 1 for a schematic of EEM production from fluorescence measurements.

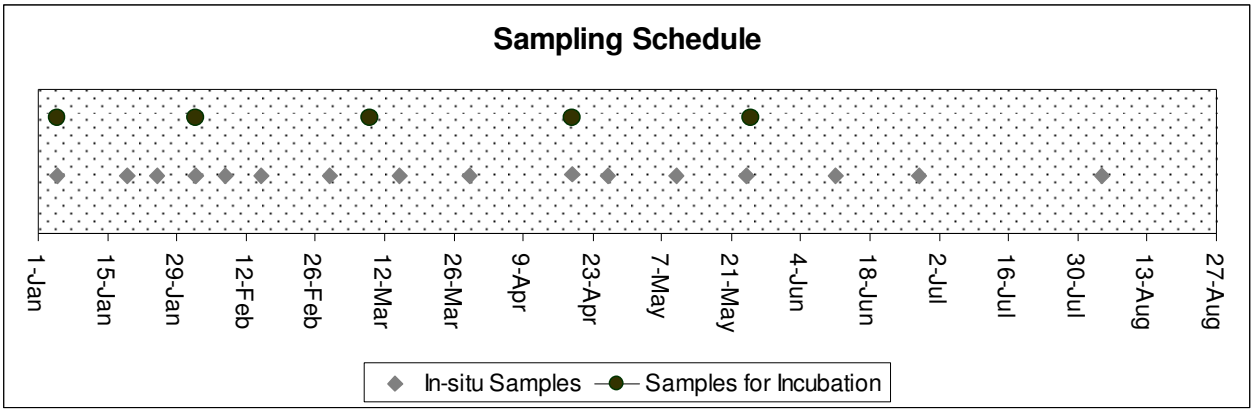

Figure 3: Schedule of samples collected in-situ. Blue dots represent samples collected for fluorescence analysis and green dots represent water collected for incubation.

Incubations

Due to constant sinking/sedimentation of POM, continuous mixing of dissolved materials, and since microbial degradation of POM and DOM sources in Lake Kinneret may continue for periods of several weeks (Hart et al. 2000, Ostapenia et al. 2009), it is not possible to track the natural degradation of any specific mass of algal POM/DOM within the lake. Instead, lake water containing natural concentrations of POM, DOM and microbes was incubated in the laboratory for a period of 3-4 weeks. This method was devised as a laboratory simulation of natural microbial processing of the POM/DOM captured in the sample. Furthermore, incubations allowed for an investigation of the relative contribution of degraded POM/DOM to fluorescence production, while controlling for differences in the initial rate of degradation of these two fractions. Based on Ostapenia et al.'s (2009) study of the relative lability of DOM/POM in a number of lakes (including Lake Kinneret), it was assumed that the amount of bioavailable organic substrate present in a sample is the sum of the labile POM and DOM, respectively. In other words, total labile organic matter (TOM_L) is the sum of labile POM (POM_L) and labile DOM (DOM_L). Incubation of unfiltered water simulated the in-situ degradation of TOM_L, while incubation of filtered water simulated the degradation of DOM_L. The degradation of POM_L was determined as the difference of these two fractions. Thus,

$$\text{If:} \quad TOM_L = POM_L + DOM_L$$

$$\text{Then:} \quad TOM_L - DOM_L = POM_L$$

Based on these assumptions, the relative contribution of labile DOM and POM to microbial production of FOM in the lake was examined in these incubations.

Samples were collected for incubation experiments on five dates (5/1/09, 8/2/09, 9/3/09, 19/4/09, 25/5/09) at station A. The February sample was lost during incubation, so only four incubation experiments were completed. For each experiment, two 5 L water samples were collected and transported to the laboratory in acid-washed jerrycans rinsed with deionized water. One sample was filtered through precombusted (550° C, 3h) Whatman GF/C glass-fiber filters to remove suspended matter, POC and algae while retaining small microbes in the sample. The other sample remained unfiltered. To correct for filtration-related reductions in oxygen concentration, filtered and unfiltered samples were left open to ambient air in high-surface-area decanters overnight in darkness to oxygenate the samples. Filtered and unfiltered samples were then bottled for incubation. The first (January) incubation took place in two 250mL glass BOD (biological oxygen demand) bottles kept in the dark at 20°C for 17 consecutive days. Bottles were sampled 4 times (about twice per week) for fluorescence analysis over the course of the incubation (see Fig. 17). The next (March) incubation used the same preparation method and was sampled 6 times over 26 days for fluorescence analysis, microbial production and microbial cell counts. March and April incubations were performed in duplicate, with one pair of samples (filtered and unfiltered) treated as above, and the other pair bottled in 12 individual 100mL glass BOD bottles. Within the 12-bottle sample series, timepoints were sampled by opening one pair of BOD bottles (filtered and unfiltered) at each sampling timepoint, ensuring that the remaining bottles remained airtight. The third (April) and fourth (May) incubations comprised 6 samples over 32 days, and 4 samples over 22 days, respectively. The fourth incubation was conducted using the 12-bottle, airtight method only. Subsamples of about 10mL were decanted into acid-washed tinted glass bottles for transport to the spectrofluorometer. Analysis of the March and April incubations, which were performed in duplicate, showed very good agreement in spectrofluorometric readings between the two incubation methods (2-bottle and 12-bottle). The 12-bottle incubation data for these two months were used for subsequent data analysis. Oxic conditions were maintained throughout the incubations; O_2 levels did not fall below the limiting concentration of 4mg/L over the course of any incubation (except day 18-25 of the April incubation).

For each incubated timepoint in the March, April and May time series (including initial lake samples), three triplicate subsamples (3 filtered, 3 unfiltered, 3 killed controls) were analyzed for bacterial production rate by the leucine uptake method described above.

Total bacterial abundance was determined by taking 5 mL subsamples from each incubation bottle and fixing these by adding 0.7mL of 5% formalin. Initially, duplicate samples from unfiltered bottles were sonicated at high power for 3 minutes on an MSE brand sonicator to shake loose attached cells into solution. A comparison among sonicated and unsonicated samples revealed that sonication yielded lower cell counts than unsonicated duplicates, suggesting that sonication may have caused bacterial cells to burst. For this reason, sonication was abandoned and sonicated samples were discarded. Formalin fixed samples in 15 ml tubes were stored in the lab at room temperature and analyzed within one month. Prior to counting, samples were vortexed and stained for epifluorescence microscopy using the DAPI method (Porter & Feig 1980). Samples were stained with a 30µL mixture of 0.2µm-filtered sterile water and DAPI (Sigma; final DAPI concentration in sample was 0.6 µg/mL), concentrated onto 25mm, 0.2µm polycarbonate (Poretics) filters, and total fluorescing cells counted using a Zeiss Axioskop UV epifluorescent microscope at 1000x magnification using a blue filter.

FOM component isolation

Three FOM components were tracked over the course of this study. Emission peaks were selected based on Borisover et al.'s (2009) PARAFAC analysis of Kinneret water. This study relied on Borisover's PARAFAC decomposition because that study benefited from a very large dataset representing a full four-season timecourse, and because individual peaks were not visually obvious in the present study's excitation/emission matrices (EEMs). The following peaks were extracted from excitation emission matrices and tracked over time in incubations and in-situ: (1) A protein-like peak (p-comp; corresponding to the fluorescent range of tryptophan) produced by excitation (Ex) at 280 nm, and emission (Em) within the range 322-382 nm. Since the shape of this peak changed both seasonally and as a result of filtration, p-comp fluorescence was calculated as the average area under the curve (AUC) in this excitation range (the sum of emission intensities in 16 consecutive 4nm bins divided by 16; Fig. 4 (c)), (2) A marine humic-like component (m-comp): Ex. 310, Em. 394. This peak was relatively flat, with a consistent, though minimal, curvature (high peak eccentricity), (3) A terrestrial humic-like component (t-comp): Ex: 350, Em: 458. The spectral shape of this peak was similar to the m-comp peak above. See Figure 4 for examples of excitation/emission plots for these three principal components. The m-comp and t-comp peaks maintained consistent shapes throughout the study (maximum emissions

were found at the same wavelength throughout the dataset), so emission intensity at a single wavelength (the maximum) was deemed sufficient to quantify each of these two components.

When working with EEMs, certain optical properties of water produce fluorescence scatter, which introduces predictable artifacts into the data matrix. Normally, these artifacts must be identified and corrected before analyzing the matrix data or proceeding with statistical analyses such as PARAFAC (Bahram et al. 2006). The two main types of scatter that must be accounted for are Rayleigh and Raman scattering. Rayleigh scatter is the elastic scattering of incident light by the water molecules. A certain fraction of all the photons emitted by the spectrofluorometer will "bounce" off of the water molecules in the sample, much like a bullet ricochets off of a surface. Some fraction of these scattered photons, which retain their wavelength and energy, will hit the fluorescence sensor and register as fluorescence. For each excitation wavelength, this produces an apparent fluorescence peak at the identical emission wavelength. In the resultant EEM, this appears as an unusually high emission peak running diagonally across the matrix at all points with identical Ex/Em. Second-order Rayleigh "echo" scattering produces a lower-intensity ridge of the same type, except that the measured "emission" wavelength is always a multiple of the excitation wavelength. For example, Rayleigh scattering of incident light with a wavelength of 300 nm could produce scatter peaks at both 300 nm and 600 nm. Raman scattering is caused by the temporary excitation of electrons in the water molecule. At each wavelength, a certain fraction of incident light will excite some electrons in the water molecule, which emit photons at a lower wavelength when they relax back to ground state. Raman scattering, which is weaker than Rayleigh scattering, is apparent in all EEMs as a diagonal signal ridge where each excitation wavelength is shifted linearly to a lower emission wavelength. The Ex/Em ranges of the fluorescence peaks tracked in this study (p-comp, m-comp and t-comp) do not fall within the range of Raman and Raleigh scattering ridges, and so no scattering corrections were necessary in this case.

To verify that the fluorescence signatures of components tracked in this study corresponded to dissolved compounds and could adequately identify changes in their concentration, and to test the sensitivity of the spectrofluorometer, a dilution was performed with Kinneret lake water on two separate dates (5/1/10 and 25/1/10). On these dates, sampled lake water was diluted in triplicate to 50% and 20% concentration using HPLC-grade water (Sigma). The samples diluted to 20% concentration were lost during transport and were not analyzed. EEMs were produced for raw lake water, lake water

diluted 50% and pure HPLC water. P-comp, m-comp and t-comp peaks were extracted from these EEMs and their intensities plotted against concentration to determine whether the fluorescence signature of these components diminished linearly and proportionally with dilution. A linear regression of component intensity against concentration was performed for each component (see figure 5 for an example).

To test for significance in fluorescent component changes over the course of laboratory incubations, a repeated measures ANOVA was performed. This statistical tool was set up such that successive samples taken within an incubation (e.g. day 1, day 3, day 7, etc.) were the repeated measure, and each independent incubation (Jan, Mar, Apr, May) was a group. This analysis was selected so that all four incubations could be compared within one ANOVA while also testing for changes over time during incubations and for an interactive effect of incubation time and incubation group. This ANOVA analysis could not be used to compare leucine uptake data from incubations because each incubation bottle was sampled for bacterial production on a different incubation day. Thus, consecutive leucine runs within each incubation were not comparable between incubations and thus could not be analyzed as repeated measures within the full (3 month) dataset. Still, Leucine uptake measures are averaged from triplicate runs, allowing for the calculation of standard deviation and testing of differences in uptake peaks and integrated uptake periods using t-tests. Statistical analyses, including regression, correlation and repeated measures ANOVA were performed using SPSS software v.12.

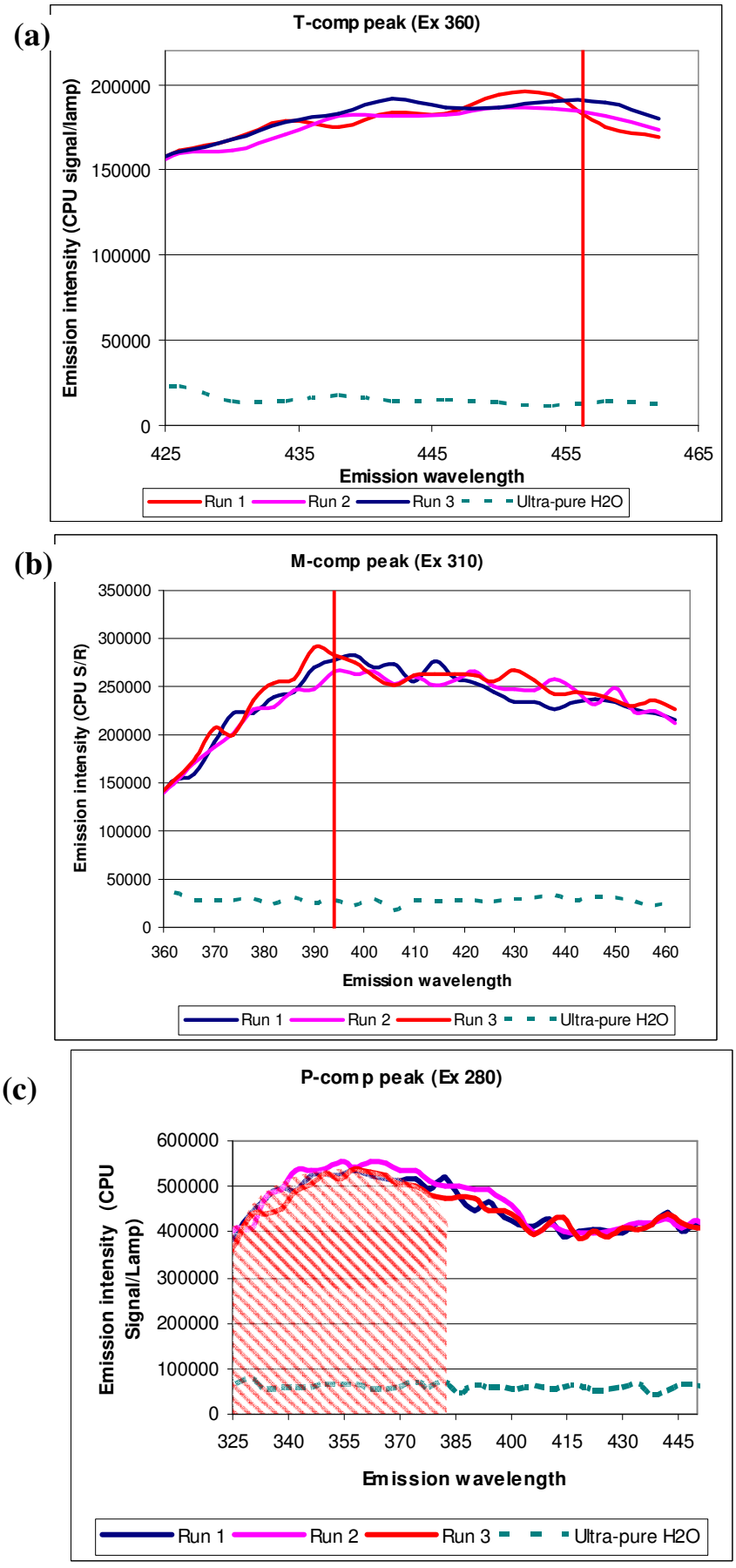

Figure 4: Example of emission spectra and peak shapes for (a) t-comp (terrestrial humic-like fluorescent component) (b) m-comp (**marine** humic-like fluorescent component) and (c) p-comp (protein-like fluorescent component) in Kinneret lake water collected on 19/4/09. Green dashed lines are control fluorescence of ultra-pure HPLC-grade water. Red lines in (a) and (b) are the wavelengths used to quantify these components. Red hatched area in (c) is the area under the curve (AUC) used to quantify this component.

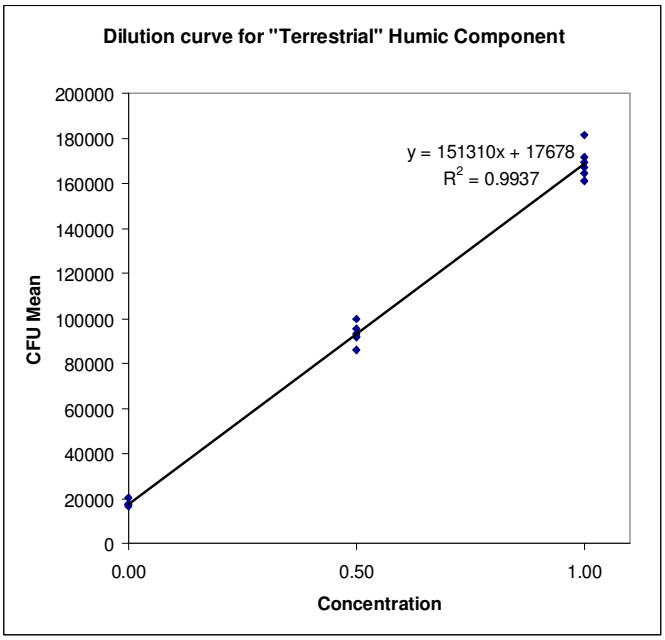

Figure 5: Example of dilution response curve for fluorescence of t-comp in water sampled on 1/5/09 and 1/25/09.

Results

Fluorescent Organic Matter

Fluorescent Organic Matter (FOM) was monitored over the 7 month period and three separate FOM components were tracked over the course of the study. Excitation of the protein-like (p-comp) fluorescence wavelength (280 nm) resulted in the greatest subsequent emission, followed by the marine humic-like (m-comp) excitation region (310 nm) and terrestrial-like humic (t-comp) region (350 nm), respectively (Fig. 6). Mean fluorescence of the marine humic-like and terrestrial humic-like components were 61% and 39% of mean protein-like fluorescence, respectively. All three components responded linearly to 3-point dilution with significant regressions between concentration and specific fluorescence (p-comp: R^2=0.922, p<0.001, a= 3.14E5, b= 7.2E4; m-comp: R^2=0.947, p<0.001, a= 2.39E5, b= 4.6E4; t-comp: R^2=0.994, p<0.001, a= 1.51E5, b= 1.7E4; see fig. 5 for an example). This indicates that the changes in fluorescence recorded over time in this study correspond to change in FOM concentration. The slope of the regression (a) defines the change in fluorescence intensity per unit change in OM concentration. The y-axis intercept of the regression (b) is not at zero, rather, it is located near the noise threshold of the instrument at the given wavelength.

From early January until the development of a strong thermocline and subsequent hypolimnetic anoxia in late April, p-comp fluorescence was highly variable, with a maximum difference (between contiguous timepoints) of 48% over 14 days. While p-comp fluctuated continuously throughout the winter production period, p-comp fluorescence values swung quickly from one tail of the sample distribution to the other (changed by at least two standard deviations) only five times, describing three maxima and two minima. The numbered arrows in Figure 6 mark these five rapid changes in p-comp concentration. Local maxima were recorded on 19/1/09, 15/3/09 and 19/4/09. To determine whether p-comp levels in this study indicate a multi-year trend in the Kinneret, a linear function was fit to the dataset. A very low and insignificant coefficient of determination (R^2 = 0.11) indicates that there was no linear trend in p-comp fluorescence over the entire study period.

Contrastingly, m-comp and t-comp fluorescence remained relatively stable throughout the winter production period. These two components were tightly coupled in-situ, demonstrating a significant positive linear relationship between them (R^2=0.71, p<0.000, N=16) for the length of the study period. All three components (p-comp, m-comp and t-

comp) demonstrated a gradual reduction in fluorescence following lake stratification (roughly mid-May to mid-June), with p-comp rising again in late summer (Fig. 6).

No discernable relationship was found between fluorescence and either Jordan river inflow or lake level during the highly dynamic winter period, though the largest rise in p-comp fluorescence began immediately after the dramatic seasonal peak in river inflow (Fig. 6).

FOM and productivity

A series of fast-paced algal production events were documented during the winter period, expressed as increases in total phytoplankton biomass and ChlA. Total phytoplankton biomass data demonstrated three local maxima (production events) of increasing intensity between lake turnover and stratification (Fig. 7). Overall, phytoplankton biomass rose by 358% between January and April before falling back to 174% of January levels in early August. The three rapid-production events, with maximum measured biomasses recorded on 15/2/09, 15/3/09 and 19/4/09, were concurrent to (or immediately following) the three peaks in p-comp (described above). A seasonal ChlA timecourse was characterized by two local maxima on 15/2/09 and 19/4/09, concurrent to the first and third peaks in phytoplankton biomass (Fig. 7). ChlA and biomass were positively correlated (One-tailed Pearson R=0.674, N=11, p=0.012). Overall, ChlA rose 175% above the initial value (1/19/09) before dropping to 51% of the initial value at the end of June. This local minimum was followed by a return to winter concentrations of ChlA towards late summer.

A significant positive linear relationship was found between total phytoplankton biomass and p-comp fluorescence for the period ranging from two-weeks post-turnover to the end of the study period (R^2=0.445, p=0.035, N=9, Fig. 8). Since fluorescence and biomass data were not obtained concurrently, some data reduction was necessary to align data from these two measures, decreasing available sample sizes in the process. Due to this reduction, the period preceding 15/2/09 showed a spurious reduction in p-comp, whereas the complete dataset described an increasing trend for this period (Fig. 8(a), Fig. 6). For this reason, data preceding 15/2/09 were excluded from this regression. Though surface ChlA and FOM were not related for the entire dataset, a significant linear relationship was also found between ChlA and p-comp when examining all data after and including the 29th of March, a local minimum in both ChlA and p-comp which preceded the second local peak in ChlA (R^2=0.60 p=0.042, N=7, Fig. 9). Reduced p-comp data preceding this date

inaccurately represented the fluorescent dynamics observed at greater temporal resolutions, and were excluded from the regression.

Secchi depth dropped from 4.2 m in January (post turnover) to 2 m in mid-March, changing in close relation to p-comp (Fig. 10). A significant negative correlation was found between Secchi depth and in-situ protein-like fluorescence over the course of the study (Pearson R=0.68). Linear regression of these metrics showed that 46% of the variance in protein-like fluorescence could be explained by changes in turbidity as measured by Secchi depth, where a 1 m increase in Secchi depth (due to reduced turbidity) corresponded to a 72078 CFU (14% from maximal) reduction in protein-like fluorescence (N= 16, R^2 = 0.48, F=11.2, p=0.005, Fig. 10(b)).

A time series of bacterial production rates was compiled for this study by combining this study's leucine uptake data with unpublished data provided by Prof. Tom Berman at the Kinneret Limnological Laboratory. Due to logistical limitations, sampling for bacterial production assays did not coincide with fluorescence sampling, so no direct correlation could be tested. Nonetheless, visual impressions (Fig. 11) suggest that increases in bacterial production track two of the three peaks observed in the fluorescence data, with one peak potentially obscured by poor temporal resolution as observed in the chlorophyll data (Fig. 7). Bacterial production declined after the onset of stratification, and rose again in late summer.

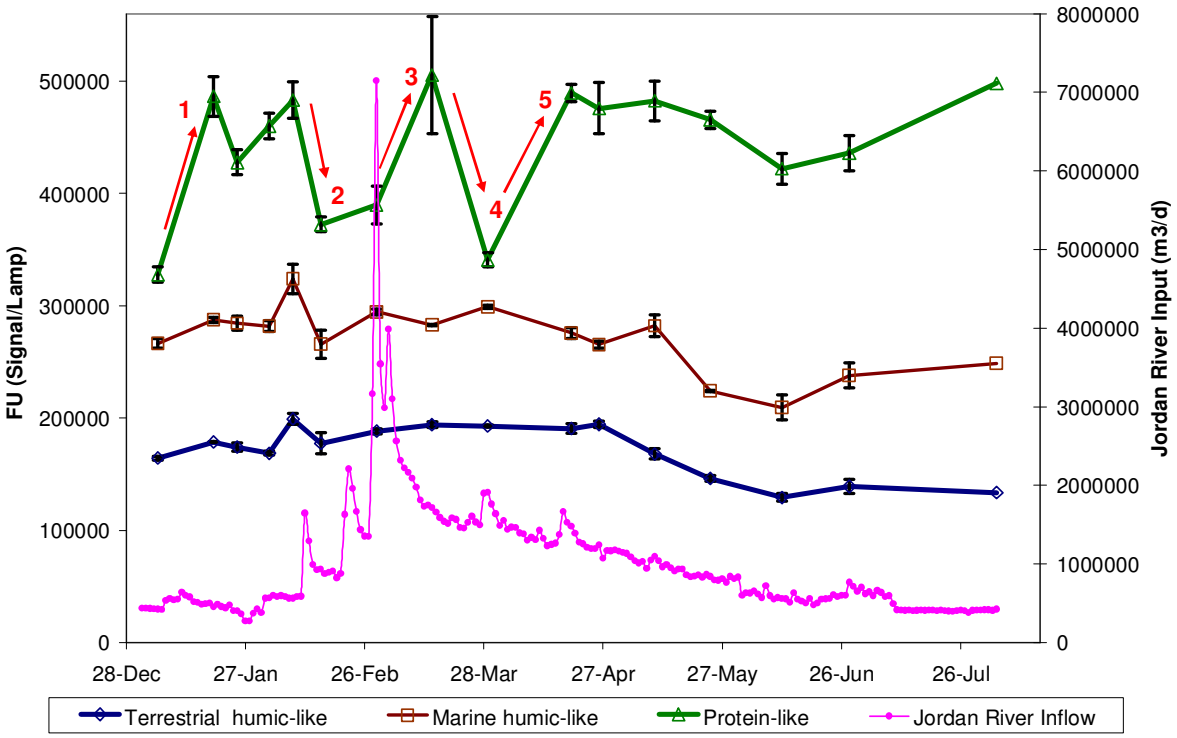

Figure 6: Lake Kinneret in-situ fluorescence intensity time series for protein-like component, marine humic-like and terrestrial humic-like components. FU = raw fluorescent units, adjusted for lamp intensity. Pink line is the volume of Jordan River input in m^3/d. Protein-like component values calculated as mean area under the curve (AUC) of fluorescence peak.

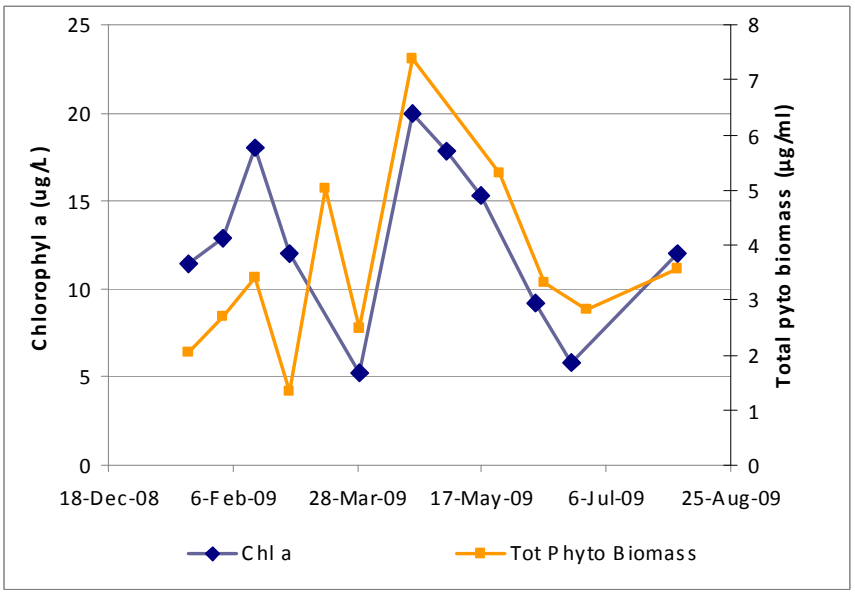

Figure 7: Time series of chlorophyll a and total phytoplankton biomass in Lake Kinneret.

a)

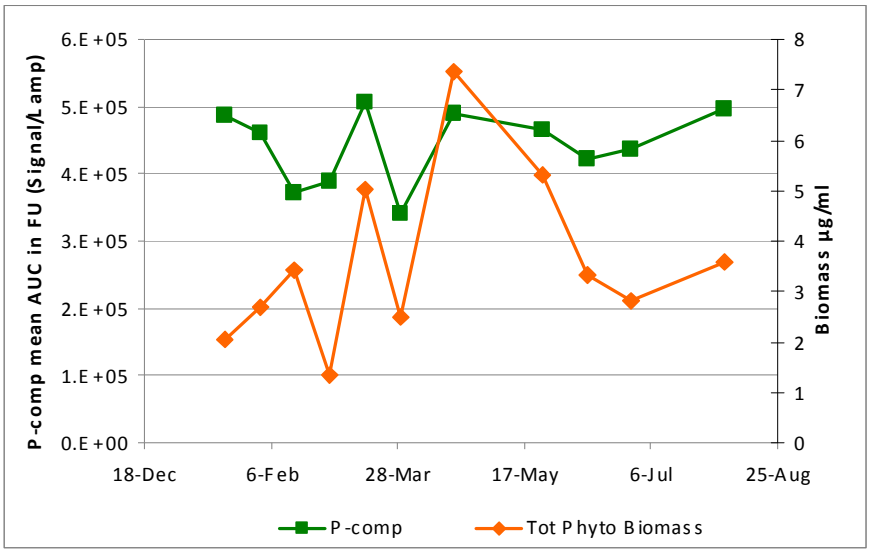

b)

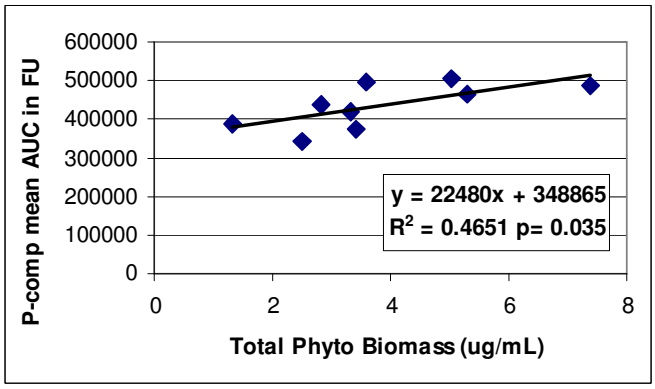

Figure 8: Time series of protein-like fluorescence (p-comp) and total phytoplankton biomass in Lake Kinneret (a) and graph of significant linear regression between these measures (b).

a)

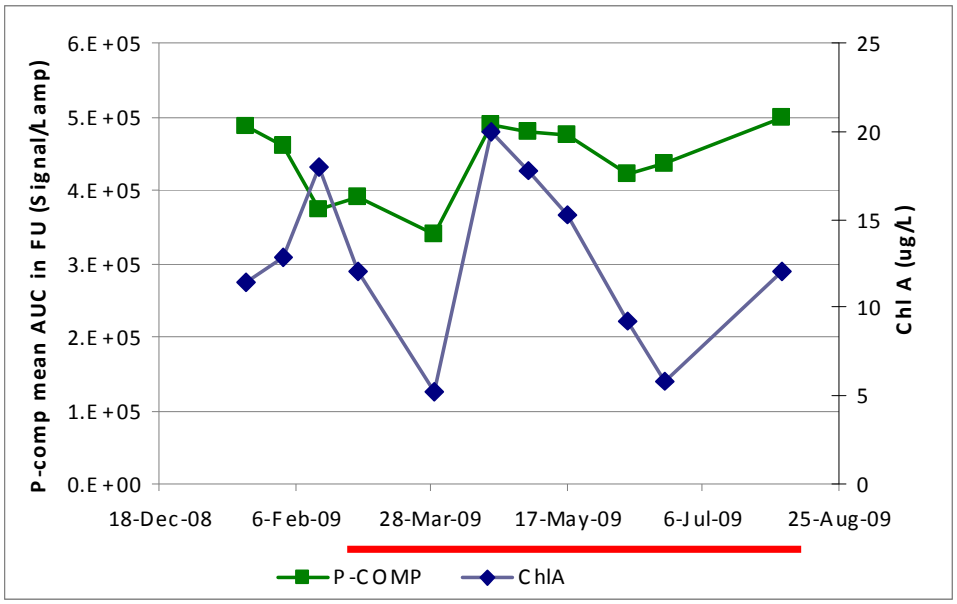

b)

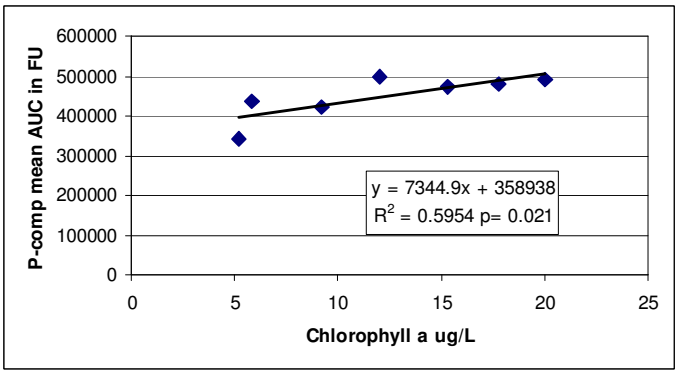

Figure 9: Time series of protein-like fluorescence (p-comp) and chlorophyll a (Chl A) in Lake Kinneret (a). Reduction of fluorescence data for correlation obscure 2 out of 3 major increases during early winter. Red line indicates sampling period for which these measures were significantly linearly related. (b) shows result of linear regression.

a)

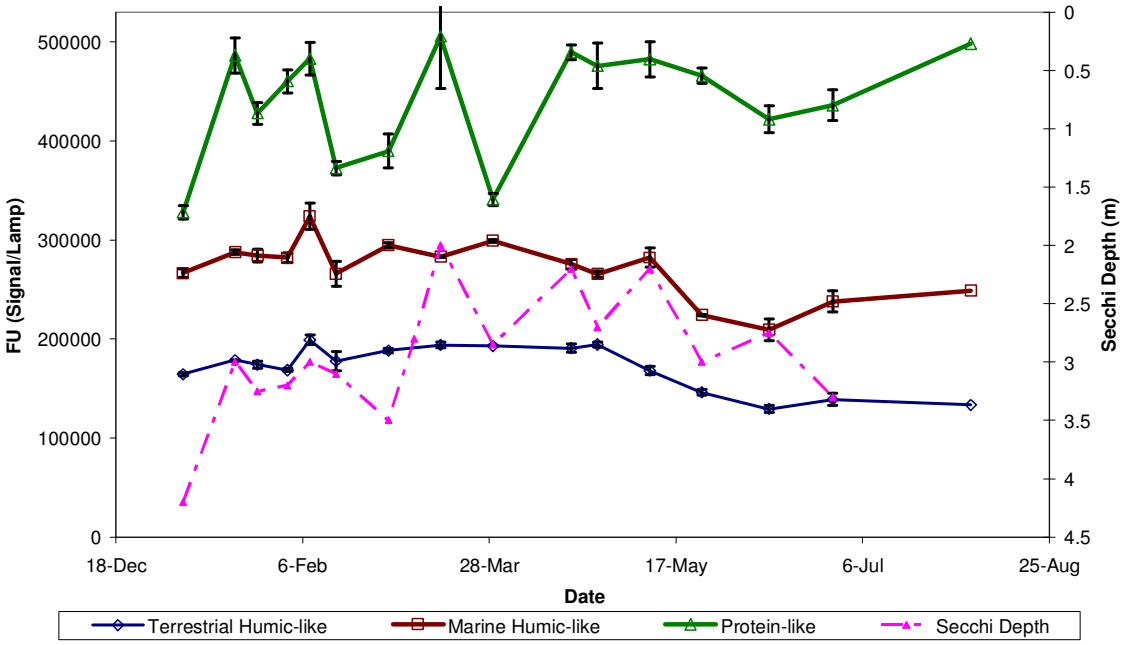

b)

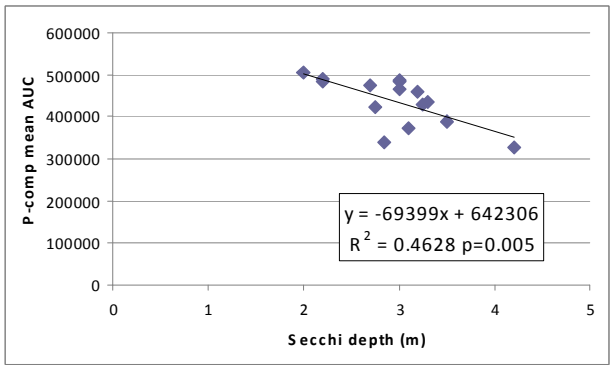

Figure 10: Lake Kinneret in-situ fluorescence intensity time series for protein-like component (p-comp), marine humic-like and terrestrial humic-like components (a). FU = raw fluorescent units, adjusted for lamp intensity. Pink dashed line is secchi depth in m. (b) A significant linear relationship was found bet. p-comp and secchi depth.

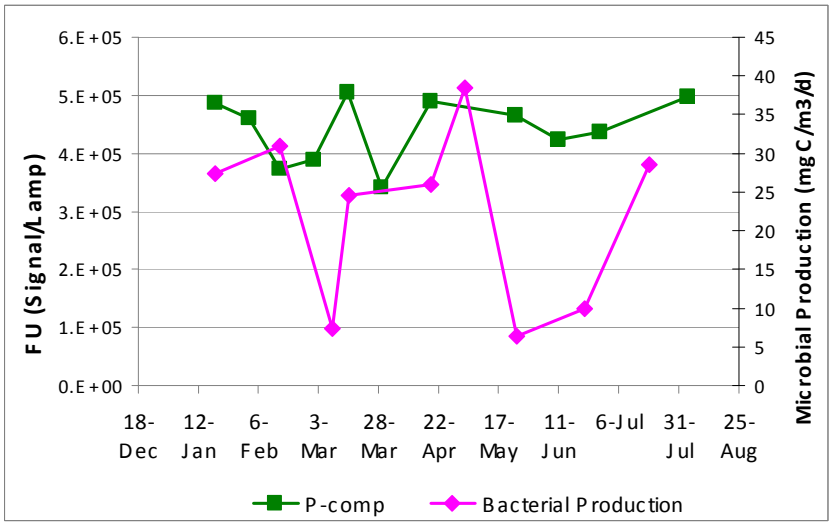

Figure 11: Time series of protein-like fluorescence and microbial productivity in Lake Kinneret.

Incubations

Incubation of lake water samples resulted in significant changes in protein-like and marine humic-like fluorescence over an incubation period of 17-22 days (Fig. 12, 13). Repeated measures ANOVA using 4-point incubation curves showed a significant main effect of incubation time for total p-comp ($p=0.006$) and total m-comp ($p<0.001$) components, meaning that the fluorescence of these components changed significantly in water that was incubated. When testing the dissolved and suspended fractions separately, p-comp showed a significant main effect of incubation time for both the dissolved ($p<0.001$) and suspended ($p=0.014$) fractions, meaning that changes in both of these fractions contributed to the overall change in fluorescence over the course of the incubations. M-comp showed a significant main effect of incubation time for the dissolved fraction ($p=0.013$) but not for the suspended fraction. This implies that changes in m-comp fluorescence over the course of incubations were primarily driven by changes in the dissolved fraction. T-comp did not exhibit any significant changes over the course of the incubations, either in unfiltered samples (total t-comp) or in the suspended fraction (unfiltered minus filtered), though a significant main effect of incubation time was found for the dissolved component (filtered samples) ($p=0.001$). P-comp exhibited greater change over the course of the incubation when compared to humic-like fluorescence. The maximum changes in m-comp and t-comp fluorescence were 44% and 30% of the maximum change in p-comp, respectively.

A significant interaction effect between incubation time and month of initial sampling was found for the total ($p<0.001$), dissolved ($p<0.001$) and suspended ($p<0.001$) fractions of p-comp, suggesting a seasonal effect. The same effect was observed in the total ($p<0.001$) and dissolved ($p<0.001$) fractions of m-comp, but not in the suspended fraction. No significant interaction effects were found for the total or suspended fractions of t-comp, though a significant interaction effect (incubation time x month) was found for the dissolved component ($p=.001$).

A significant between-subject effect of incubation month was observed in the total ($p=0.006$), dissolved ($p=0.005$) and suspended ($p=0.022$) fractions of p-comp. Post-hoc Tukey's tests found that for raw (unfiltered) samples, the total change in p-component (Δp-comp) during the April incubation was greater than during the March and May incubations ($p=0.006$ and $p=0.016$ respectively). The same relationships were found in the suspended fraction ($p=0.02$ for April>March and $p=0.098$ for April>May). In the dissolved fraction, Δp-comp in the April incubation was significantly greater than Δp-comp in the January

(p=0.005) and May (p=0.025) incubations. Δp-comp in the January incubation was greater at a borderline significance level than Δp-comp in the March incubation (p=0.061). Contrasts in Δp-comp between incubation months are summarized in Figure 12.

A significant between-subject effect of incubation month was observed in the total (p=0.001), and suspended (p=0.018) fractions of m-comp, and a trend-level effect of month was found for the dissolved component (p=0.067). Post-hoc Tukey's tests found that the increase in total m-comp fluorescence during the April incubation was greater than the increase in the January, March and May incubations (p=0.003, p=0.012 and p=0.001, respectively). In the suspended fraction, Δm-comp for April was significantly greater than Δm-comp for May (p=0.018). In the dissolved fraction, Δm-comp for May was greater than Δm-comp for January, though only at the trend level (p=0.056). Contrasts in Δm-comp between incubation months are summarized in Figure 13.

No significant effect of incubation month was found with respect to the terrestrial humic-like component (all fractions). This suggests that this component behaved similarly over the course of all four incubations. Figure 14 shows Δt-comp values for each incubation month.

Microbial Productivity in Incubation

Microbial carbon production, as measured by uptake of radiolabelled leucine, showed a roughly 200% increase in total productivity (area under the curve of incubation) from the March incubation to the May incubation. The majority of this increase was attributable to the suspended fraction of incubated water (Fig. 15). Total productivity remained high through the end of May. A comparison of productivity time courses within the April and May incubations reveals an early spike in production in unfiltered samples during the May incubation, and faster ramping-up of production in both filtered and unfiltered treatments as compared to the April incubation. DAPI counts of microbial cell densities showed extremely high inter-replicate and inter-sample variability with no significant or apparent trend or correlation. These data were not instructive and were therefore excluded from further analyses.

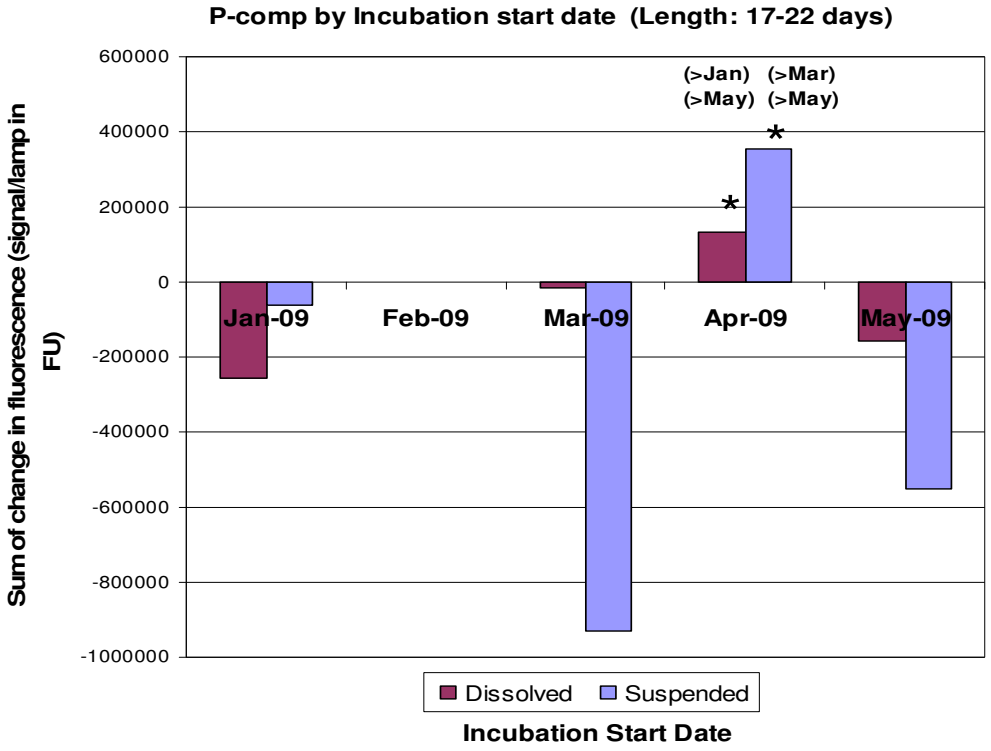

Figure 12: Change (AUC minus baseline) in protein-like fluorescent component (p-comp) over the course of incubation for four independent incubations beginning in Jan, Mar, Apr and May. Production/consumption attributable to dissolved (filtered incubation) and suspended (unfiltered incubation minus filtered) fractions are shown separately. P-comp was consumed in all incubations apart from the April incubation, in which p-comp was produced. Post-hoc tests of repeated measures ANOVA show that values for April are sig. different from values in all other months.

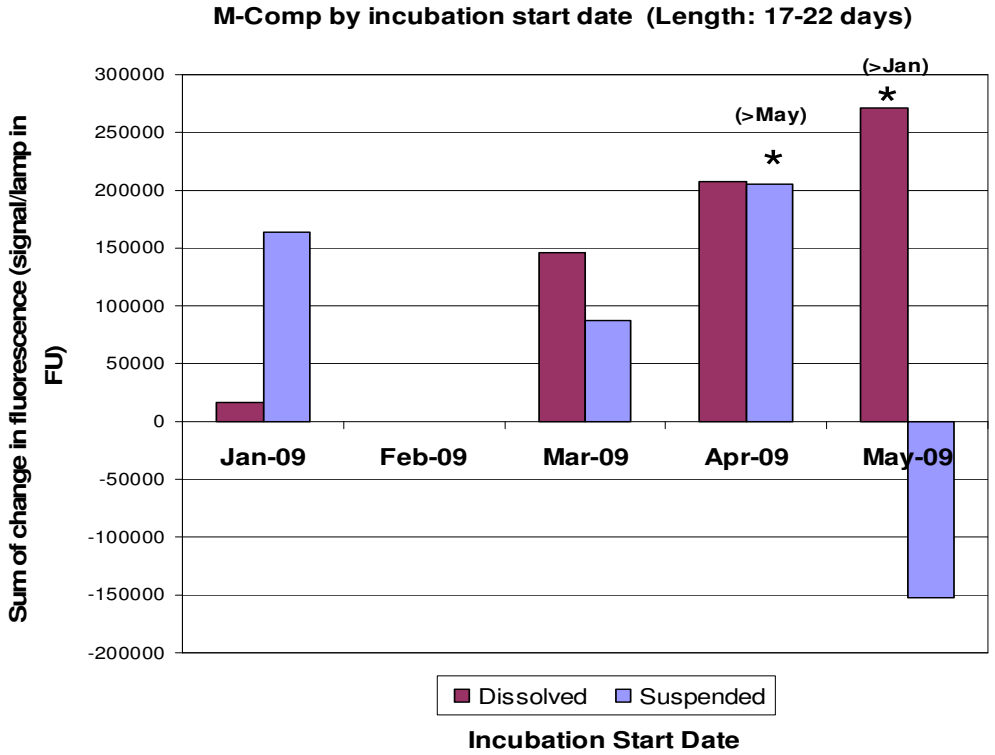

Figure 13: Change (AUC minus baseline) in marine humic-like fluorescent component (m-comp) over the course of four independent incubations. Production/consumption attributable to dissolved (filtered incubation) and suspended (unfiltered incubation minus filtered) fractions are shown separately. M-comp was produced in all incubations. Post-hoc tests of repeated measures ANOVA show that values of total change for April are sig. different from values in all other months, and suspended values for April and dissolved values for May are sig. different from corresponding (suspended or dissolved) values in May and January, respectively.

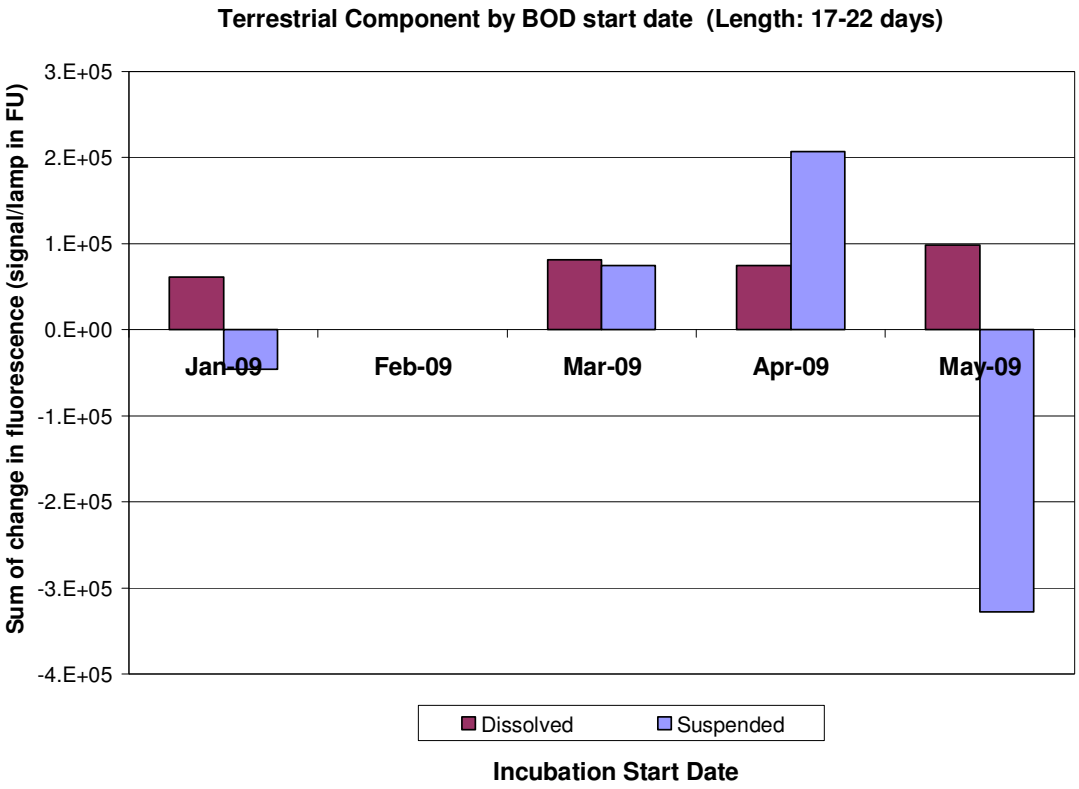

Figure 14: Change (AUC minus baseline) in terrestrial humic-like fluorescent component (t-comp) over the course of four independent incubations. No significant changes were found in t-comp concentrations over the course of the incubations when testing using a repeated measures ANOVA.

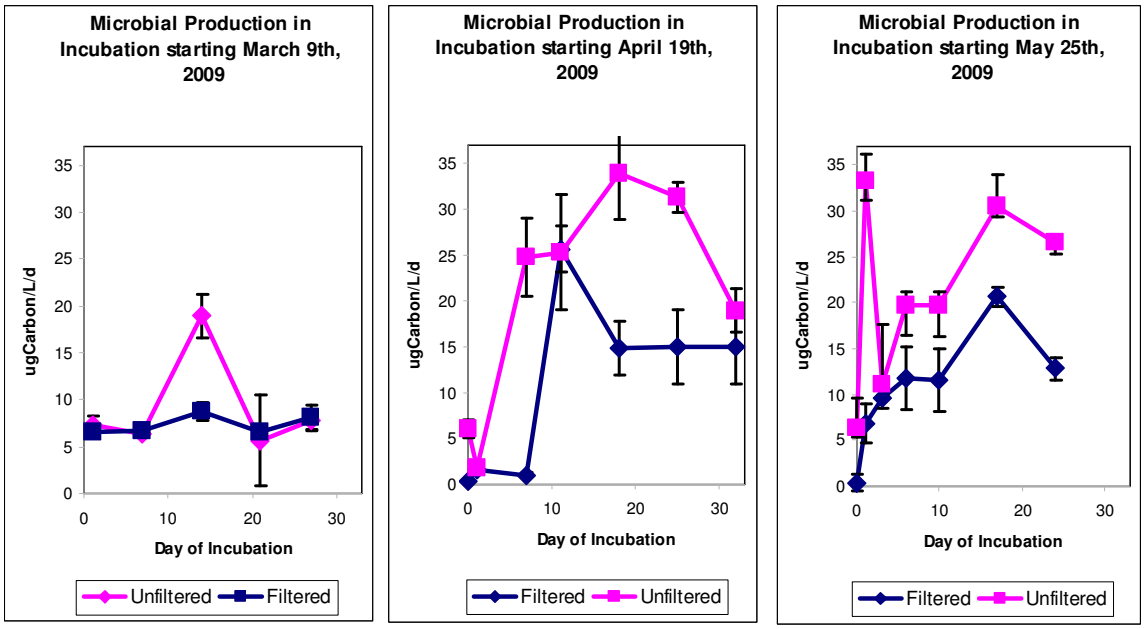

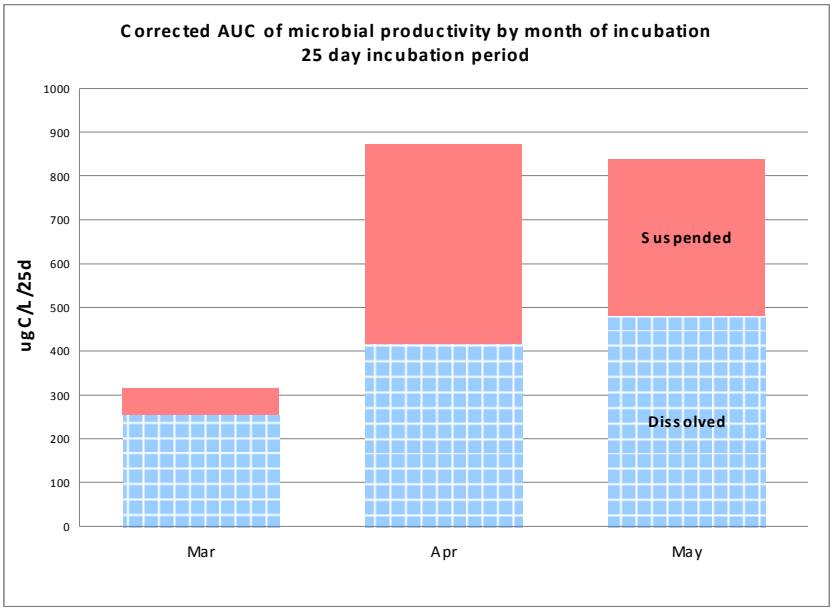

Figure 15: Microbial carbon production in incubation by month. Microbial production in unfiltered (pink line) and filtered (blue line) incubations are shown separately. Contrasts are summarized in stacked bars representing total AUC of microbial production for dissolved (filtered incubation) and suspended (unfiltered minus filtered) incubations.

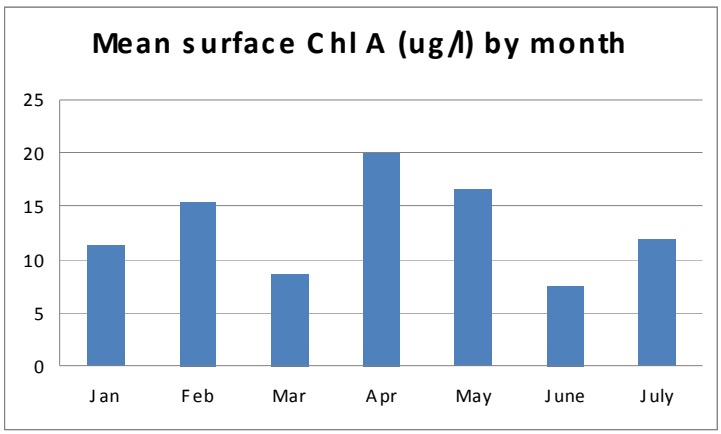

Figure 16: Mean chlorophyll a concentration by month for Jan-July 2009.

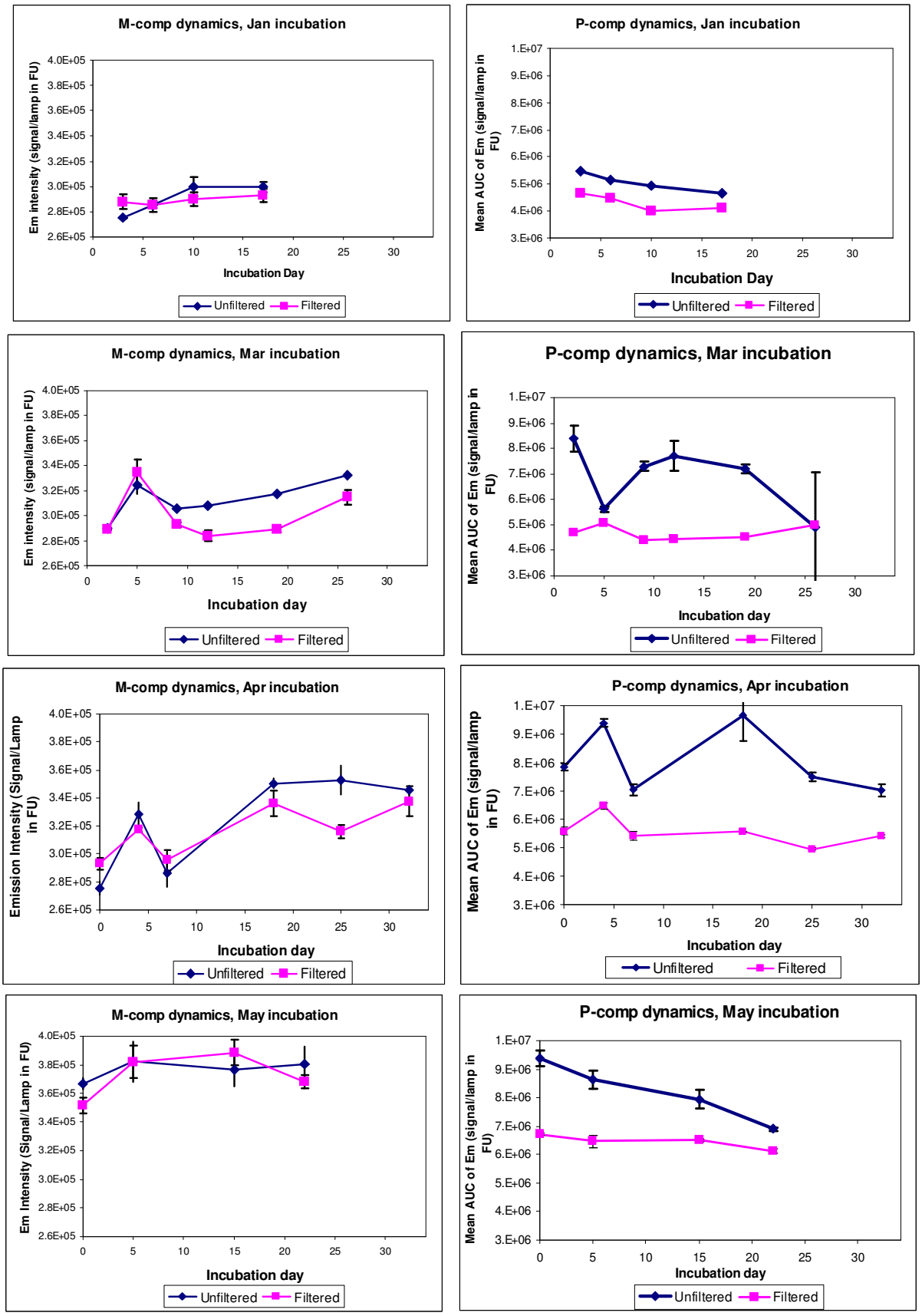

Figure 17: Raw fluorescence measures for protein-like (p-comp) and marine humic-like (m-comp) FOM in four separate incubations starting in Jan, Mar, Apr and May.

Discussion

This study attempts to relate seasonal changes in primary production and microbial activity to fluorescent organic matter (FOM) concentrations in a lake ecosystem. Data were collected from Lake Kinneret, Israel throughout a nine-month period at a finer resolution than has previously been documented in this water body. Short sampling intervals were chosen in an attempt to identify rapid responses of the in-situ microbial community to phytoplankton production events. Samples were collected more often during the winter/spring period so as to capture rapid changes in production (blooms), and unamended lake water incubations were employed to track FOM change during microbial degradation of particulate and dissolved organic matter (POM and DOM, respectively).

Productivity and fluorescence in Lake Kinneret

While *Peridinium gatunase* was the dominant species in Kinneret phytoplankton blooms for decades, the relative contribution of this dinoflagellate to yearly phytoplankton production has become unpredictable since the year 2000 (Zohary 2004). Specifically, the winter/spring season of 2009, when this study took place, did not include a major *P. gatunense* bloom. Instead, between February and May, a number of smaller phytoplankton production events provided stepwise boosts to phytoplankton biomass (Fig. 7). This production period (Feb-May) was dominated by chlorophytes, which contributed about 50% of the total wet-weight biomass, as well as dinoflagellates of the genus *Peridiniopsis*, (20-30%) and several species of cyanobacteria (mostly *Microcystis aeruginosa*). The Cryptophyte *Cryptomonas* also made a significant contribution to algal biomass in January (34%) and February (10-28%) but then declined to 3-5% of the total biomass (Zohary, personal communication).

In this study, production peaks in these taxa were reflected in local peaks (representing threefold or fourfold increases) in total phytoplankton biomass, and to a lesser extent in ChlA concentration (Fig. 7). While biomass and Secchi depth captured three major high-productivity bloom events pre-stratification (Fig. 10), chlorophyll data revealed only one major rise. This disagreement may be an artifact of the low temporal resolution of ChlA,

since in a previous twenty-year study in the Kinneret, ChlA and biomass have been well-correlated within a given year (Berman et al. 1992). The microbial community responded to two of these bloom events, with a 240% rise in carbon production in April and a further 50% increase in early May, though the May peak in microbial production lagged approximately two weeks behind the largest of the spring production peaks (Fig. 11). I hypothesize that this lag reflects a period of DOM accumulation, phytoplankton cell senescence and microbial reproduction. Subtraction of filtered incubation production from unfiltered incubation production suggests that up to 52% of integrated microbial carbon production originated from the particulate fraction, though this value does not differentiate between fresh POM and POM that was degraded over the course of the incubation.

While p-comp fluctuated continuously throughout the winter production period, p-comp fluorescence swung more than one standard deviation from the mean only five times, describing three maxima and two minima (Fig 6). This suggests that there were three major p-comp production/addition events in the lake, and two major consumption/reduction events. The small and insignificant coefficient of determination ($R^2 = 0.11$) of linear regressions in these data indicates that there was no overall trend in p-comp fluorescence over the entire study period. Thus the winter production period (Jan-April) was highly dynamic, characterized by three major swings in this component. A modest, roughly month-long decline in all three measured components (p-comp, m-comp and t-comp) was discernable a few weeks after the onset of stratification (mid-May), potentially reflecting a seasonal export of these dissolved components to below the upper mixed layer, though this trend was reversed in early summer as all three components began to rise in mid-June.

In this study, high-production events were accompanied by increases of up to 48% in the p-comp of the FOM pool, suggesting that p-comp is produced in the water column during fast-paced phytoplankton growth, either as exudates from living cells or as the product of microbial consumption or decomposition of exudates and senescent cells. This finding reinforces the results of (Stedmon & Markager 2005b), which showed that increases in protein-like fluorescence were related to exponential phytoplankton growth in seawater mesocosms**.** The relationship between the p-comp and primary productivity is strengthened by significant positive linear relationships between this component and total

phytoplankton biomass, ChlA and Secchi depth (Figs. 8-10). ChlA and p-comp contemporaneously tracked 1 out of 3 bloom events observed during the sampling period, and were linearly related from just before the onset of this bloom until the end of the study period. Also, a decreasing post-stratification (June-July) and increasing midsummer (July-August) trend was apparent in p-comp, ChlA, phytoplankton biomass and microbial productivity (Figs. 8-11).

The parallel dynamics of p-comp and phytoplankton primary production (as indicated by the proxies of biomass, ChlA and Secchi depth) indicate that there is a relationship between these two factors, though the expression of this relationship was somewhat obscured by low temporal resolution or reduction of the data for statistical purposes in my data set. Notably, the full p-comp time series (N=17) demonstrated three major peaks (Fig. 7), whereas data reduction of the p-comp series (N=11) to match only those dates on which samples were also taken for ChlA captured only 1 peak (Fig. 9). It is notable that Zhao et al. (2009) found a strong in-situ relationship between total CDOM absorbance (and fluorescence) and ChlA, but only during estuarine algal blooms and not during non-blooming conditions. This relationship was also observed in N and P amended mesocosms (Stedmon & Markager 2005a). Chen et al. (2004a) and Borisover et al. (2009) did not find a statistically significant relationship between ChlA and FOM. Since chlorophyll a concentration is a rough measure of photosynthetic capacity and does not measure production *per se,* changes in ChlA may not be a good measure of fine scale changes in autotrophic activity. Subsequently, ChlA may only correlate with p-comp during periods of dramatic algal population growth.

This study provides evidence of fine-scale, highly dynamic in-situ responses of protein-like DOM to measured in-situ changes in lake productivity. While at least one previous incubation study has found dramatic fine scale increases in FOM, this involved nutrient amendments (Stedmon & Markager 2005) and in-situ studies have primarily reported significant FOM variability on timescales of weeks to months (Stedmon & Markager 2005; Borisover et al. 2009). These findings suggest that further studies of in situ CDOM dynamics should strive to minimize sampling intervals, in an effort to recognize the true dynamics of CDOM concentrations in natural systems. At higher temporal resolutions, protein-like fluorescence may prove useful as an additional, relatively easy and

inexpensive tracking marker for overall primary production in aquatic systems. In a series of 28 Canadian lakes representing a range of trophic conditions, Cammack et al. (2004) found that tryptophan fluorescence was an excellent predictor of bacterial growth, bacterial respiration and total plankton respiration, performing better than the concentration of bulk DOM. The present study reinforces the potential of protein-like fluorescence to serve as a simple monitoring tool for lake trophic dynamics by adding phytoplankton growth to the list of trophic parameters to which p-comp fluorescence is sensitive.

Although p-comp fluorescence fluctuated considerably, the terrestrial humic-like fluorescent component (t-comp) remained steady throughout the winter production period (Fig. 6), dropping only after stratification set in. Strong t-comp signals have been found in rivers and streams, specifically where the catchments are rich in organic deposits such as forests and wetlands (Stedmon et al. 2003, Kowalczuk et al. 2003, Baker & Spencer 2004). In this study, t-comp concentrations did not change significantly in incubations of Lake Kinneret water, suggesting that this fluorescent component is neither consumed nor produced in the water column of Lake Kinneret. While both p-comp and m-comp were produced in incubation, the lack of observed t-comp production reinforces its characterization as "terrestrially derived" fluorescent material. A dataset-wide main effect of incubation time was identified by the repeated measures ANOVA in the dissolved fraction (filtered samples) only, but since the total and suspended fractions of t-comp did not change significantly over the course of the same incubations, I consider this to be a spurious statistical result. While oceanic and estuarine FOM studies (Coble 1996, Stedmon C.A. et al. 2003, Kowalczuk et al. 2003, 2009, Murphy et al. 2008) have successfully used terrestrial fluorescence (identified by PARAFAC or peak-picking) to track riverine inputs into bays and estuaries, t-comp was not found to relate to terrestrial input (as measured by Jordan River inflow) in this study. This suggests that the majority of t-comp inputs to Lake Kinneret may be the result of FOM production within lake sediments as opposed to terrestrial runoff rich in soil leachates or plant detritus. Borisover et al.'s (2009) identification of near-bottom t-comp accumulation during summer stratification also supports a sedimentary source for this component in the Kinneret, since runoff or riverine input would be restricted to the wet winter period. The unmonitored subsurface saline springs which feed into the Kinneret are another possible source of terrestrial DOM,

though water and solute input from these springs appears to track lake level (Rimmer & Gal 2003), which should produce a stronger wintertime (as opposed to the observed summertime) signal of t-comp accumulation. This suggests that the springs, many of which have already been diverted (Kolodny et al. 1999), are unlikely to represent a majority input of t-comp into the lake.

Despite successful validation of component signatures using dilutions, it was not possible to test for or eliminate the potential for quenching effects within these samples. By quenching effects, we refer to the potential for one fluorophore's emitted fluorescence to be absorbed in the excitation of another fluorophore, thus quenching the first component's signal (Udenfriend 1962). In this study, p-comp fluorescence was at particular risk of quenching, since emissions at 322 µm were very close to the m-comp excitation peak at 310 µm. In other words, within a given water sample, some of the fluorescent emission from the protein-like component may be absorbed by the marine humic-like component, resulting in a weaker p-comp fluorescence signal and a stronger m-comp signal. Previous spectrofluorometric studies of natural waters have largely ignored potential quenching effects, perhaps due to the difficulty in controlling for this factor. In order to determine a proper quenching correction, the "overlapping" fluorophores must be physically isolated and their respective fluorescence assessed in the absence of interfering quenchers. For quenching fluorophores which are incorporated into compounds with differentiable masses, methods such as solid-phase microextraction, centrifugation, column extraction and ultrafiltration may be able to physically separate quenching components. Alternately, a few complex methods such as time-resolved fluorometry (Maji et al. 2000) have been devised for correction of quenching effects, but these require a great deal of expertise. Fluorescent components in this study were composed of diverse complex molecules with varying sizes and masses and could not be separated physically, therefore it was impossible to prevent or isolate internal quenching effects. Still, in the case of p-comp quenching by m-comp, it is unlikely that m-comp was able to significantly affect the much stronger protein-like component signal. Moreover, since p-comp fluorescence was determined by taking the area under the curve (AUC) of the wider protein-like peak, low-wavelength quenching effects would be mitigated somewhat by the inclusion of higher wavelengths in the AUC. In the inverse case, we may ask whether p-comp emissions confounded the m-comp signal as a result of internal excitation, but this is also unlikely

since m-comp and p-comp were not correlated over the course of this study, meaning that strong p-comp emissions did not predict any increase in m-comp excitation. Moreover, since quenching rate is directly dependant on the concentration of quenching fluorophores in the sample, dilution of samples should result in variable quenching rates, wherein more dilute samples would suffer less quenching. Thus, if quenching were significantly reducing the fluorescence of the p component, a p-comp dilution curve should bend upwards towards the more dilute end of the graph, where m-comp concentrations (and subsequent quenching) are lower. M-comp dilution curves should show a mirror-image trend, bending upwards as concentrations reached 100% and more p-comp emission was available to excite the m component. Neither of these deviations were apparent in the dilution curves of p-comp and m-comp, which showed high linearity (R= 0.92 & 0.95, respectively). Therefore, it is unlikely that significant quenching effects are confounding the present study's dataset.

FOM and the microbial community

This study found that while phytoplankton productivity is tracked by p-comp in Lake Kinneret, autotrophic production may not be the primary source of protein-like FDOM in this system. Several studies have related CDOM absorbance (Nelson et al. 2004b), and more specifically, protein-like (Cammack et al. 2004, Hudson et al. 2008) and marine humic-like (Nieto-Cid et al. 2006) fluorescence to microbial processing of organic matter. In this study, p-comp probably reflects microbial processing of phytoplankton-produced biomass, since the major source of OM in the lake is phytoplankton. A seasonal time series of microbial production in this study (Fig. 11) indicates that microbial production responds to increases in phytoplankton biomass, which are also tracked by temporal changes in p-comp fluorescence.

A recent study by Berman et al. (2010) has found that between the years 2000-2007 in Lake Kinneret, monthly bacterial growth efficiency fluctuated widely (from 15%-81%), but that when data were averaged over 6-month periods this variability diminished considerably. Berman et al. (2010) hypothesize that this difference in apparent microbial growth rates may be caused by short-term fluctuations in bacterial substrate availability. This study found that while p-comp fluorescence showed no general trend over the course

of the seven month sampling period, p-comp fluctuated widely on shorter timescales during the winter production period (Fig. 7). If microbial degradation/production regulates the concentration of p-comp in the Kinneret, then rapid cycles of p-comp production and destruction may indeed reflect these hypothesized fluctuations in the availability *or lability* of microbial substrates. Further study is required to examine the relationship of these rapid fluctuations in p-comp fluorescence to the accumulation and degradation of protein-like DOM. Moreover, it remains to be seen whether these rapid fluctuations are found in other lakes with varying rates of OM loading and microbial production.

Further evidence of microbial processing of FOM was obtained in dark incubations, where p-comp and m-comp fluorescence exhibited changes over the course of three weeks of light limitation. Dark incubations were used to control for photosynthesis, ensuring that FOM changes were not influenced by phytoplankton growth and that the algal biomass available for microbial processing reflected natural lake concentrations at the time of sampling. Significant changes in m-comp and p-comp were recorded over time for incubations of filtered water, representing a highly variable fraction of the total (unfiltered, baseline-subtracted) changes in p-comp and m-comp fluorescence. Changes in filtered water accounted for as little as 2% and as much as 100% of the total changes in these components, depending on month of incubation. These values suggest that the relative importance of DOM concentrations during FOM production and/or consumption is unpredictable, and may change seasonally in response to changing DOM/POM composition and loading. In the May incubation, for example, the fraction of total m-comp production (in unfiltered water) attributable solely to DOM (as measured in filtered water) was dramatically greater than in January (see Fig. 13). In other words, the ratio

$$\Delta\text{m-comp} \mid \text{filtered} : \Delta\text{m-comp} \mid \text{unfiltered}$$

was much higher for May than for January. This increase in the relative contribution of DOM in m-comp production may reflect fresh DOM inputs related to the spring bloom. It is important to note that filtration of particulates from incubation samples also removes attached bacteria from those samples. This means that comparisons between the dissolved and suspended fraction necessarily also compare samples which differ in total microbial biomass (a result of the removal of POM-attached microbes.) Since sonication was unable

to shake attached microbes loose without causing lysis, there was no effective way to control for microbial biomass between comparisons. Still, these comparisons should accurately represent the differences in total fluorescence production between attached populations' processing of POM and free-swimming populations' processing of DOM.

Microbial activity was also reflected in significant FOM changes in unfiltered samples. Subtraction of filtered incubation samples' ΔFOM values from unfiltered values suggests that microbial decomposition of POM (including phytoplankton cells, detritus and other suspended particles) is highly variable, accounting for 19-98% and 38-91% of the summed changes in p-comp and m-comp fluorescence, respectively. These values should be treated with caution, since microbial processing of dissolved and particulate organic matter may not be additive processes (Parparov, personal communication) as was previously assumed (Ostapenia et al. 2009). In the May incubation, for example, filtered samples demonstrated a greater accumulation of m-comp than unfiltered samples. This challenges the previous assumption that total fluorescence production is driven by the availability of both DOM (as measured within filtered samples) and POM (as measured by subtracting values in the filtered sample from values in the unfiltered sample). The higher fluorescence values in the filtered (DOM only) samples suggest that the suspended fraction may have been responsible for either a net consumption (as opposed to production) of m-comp in this incubation, or that the suspended fraction may have mitigated m-comp production through, for example, increased availability of alternative substrates. Moreover, while POM remained available to microbes in aerobic conditions throughout the incubations, POM in the lake is eventually deposited in sediments and/or descends into the anoxic hypolimnion during the stratified season, exposing this material to entirely different microbial communities and processes. While previous studies have found POM to be significantly more labile than DOM in lake systems of varying trophic states (Ostapenia et al. 2009) including the Kinneret (Parparov, unpublished data), this study suggests that the relative lability of POM and DOM, at least with respect to the fluorescent fraction, may vary widely over the course of the year.

M-comp and p-comp fluorescence was found to successively increase and decrease over the course of some incubations (Fig. 17), suggesting that both components' concentrations are controlled by opposing processes of production and consumption or decomposition.

Accumulation of both components was significantly higher in April than in other months, and integrated microbial production also increased threefold in April relative to March. ChlA and phytoplankton biomass concentrations (Fig. 7, 16) both reached their seasonal maximum in late April, implying that the April incubation contained the highest concentration of phytoplankton biomass of all incubations. Thus, p-comp and m-comp accumulation (and microbial production) in incubations was positively related to phytoplankton biomass in the April samples. This reinforces and expands the results of previous studies, which showed that protein-like fluorescent components could be either produced or consumed in incubation, depending on the level of primary production (Nieto-Cid et al. 2006) or the availability of labile DOM (Nelson et al. 2004). For m-comp, which accumulated in every incubation, the relative importance of DOM over POM in fluorescence accumulation (as measured by the ratio of fluorescence increase in *filtered* versus *unfiltered minus filtered* samples) increased from Jan to May. For p-comp, which was consumed in every incubation apart from April, DOM was a relatively small influence on FOM change in every month except for January. Accumulation and removal of p-comp in incubation were primarily driven by the influence of the suspended fraction (see Fig. 12). This strengthens in-situ findings relating p-comp and phytoplankton biomass, since phytoplankton made up a large fraction of the POM in these incubations.

Though m-comp accumulated in all of the incubations, lake measurements did not show significant accumulation of m-comp in-situ. Seasonal changes in lake m-comp levels were negligible, indicating that m-comp production in incubation is not reflected in-situ. This discrepancy may result from an unidentified process of m-comp removal in-situ, rather than a lack of production. Stedmon et al. (2003) found that photodegradation is an important sink for microbially-derived humic material, which suggests that this process may remove newly produced m-comp in the Kinneret before it can accumulate in the upper mixed layer. Borisover et al (2009) found that the concentration of humic components in the Kinneret was best predicted by the depth below the water surface; humic concentrations were greater at depth regardless of the distance from the lake bottom. Since photochemical processes such as photobleaching decrease uniformly with depth (along with light penetration), this finding strengthens the hypothesis that light-dependent processes are controlling the concentration of m-comp in the Kinneret. These processes may include simple photobleaching, or post-irradiative increases in lability

leading to rapid CDOM bio-degradation (Moran & Zepp 1997). Nieto-Cid et al. (2006) found that in low-salinity productive coastal/estuarine waters, marine humic FDOM concentrations increased with depth, while surface waters were enriched in protein-like FDOM. Using a combination of short (1 d), unamended dark and light incubations, these authors found a positive correlation between photodegradation of dissolved marine humic substances and bacterial production. This was interpreted as evidence of rapid photodegradation of recently produced marine humics and subsequent rapid metabolism of photodegradation products by the bacterial community. In other words, humic substances produced during bacterial metabolism in the dark were quickly degraded and consumed after exposure to sunlight. This further supports our hypothesis that photodegradation effectively quenched the in-situ m-comp production signal in this study, despite our finding that m-comp was produced in every incubation. Borisover et al (2009) suggested that oxidation may also play a role in reducing humic FOM concentrations, but no reduction in m-comp fluorescence was observed in the present study's incubations, where O_2 remained above 4 mg/L during reported intervals (Parparov, unpublished data). Thus, photoreactive processes remain the most likely mediator of m-comp fluorescence in-situ, despite the fact that some studies have found CDOM of microbial origin to be minimally photoreactive (Chen et al. 2004).

Rosenstock et al (2005) conducted a series of incubation studies using Sargasso sea water which suggest an interesting chemical mechanism to explain some of the FOM dynamics observed in my study. In samples containing high concentrations of *humic-bound* dissolved amino acids, UV-irradiation stimulated increased glucose uptake and release of dissolved *free* amino acids when compared with dark controls. Conversely, irradiation reduced this uptake and release at low concentrations of humic-bound amino acids. This suggests that photodegradation may mask new production of marine humics by rapidly degrading the labile, newly produced humic substances and unbinding bacterially bioavailable amino acids. Meanwhile, a baseline concentration of refractory humics remains behind. This would support a production-related fluorescence signal that begins as m-comp but shifts rapidly away from the m-comp fluorescent range and into the p-comp range as amino acids are released during photodegradation. These amino acids would subsequently serve as growth substrates for the microbial community, resulting in a production-correlated peak (and subsequent decline) in p-comp fluorescence, as observed

in this study. Though theoretically plausible, this mechanism requires testing in the Kinneret.

Further research is recommended to clarify FOM dynamics in Lake Kinneret. First, a comprehensive PARAFAC analysis of the present dataset would support the component peaks described by Borisover et al. (2009) and may more precisely establish spectral boundaries for shape-shifting peaks such as the p-comp signal tracked in this study. Despite the suggestion that filtration does not significantly affect fluorescence in Kinneret samples (Borisover, pers. communication), this study found that POM-sourced fluorescence may be a significant component of the total fluorescence signal irrespective of the DOM pool (see Figures 12, 13, 17). For this reason, future studies should measure the fluorescence of both filtered and unfiltered in-situ samples to separate the FOM signatures of POM and DOM. Future incubation studies would benefit from parallel treatments of dark and sunlight-exposed incubations to examine the effect of photodegradation on the fluorescence and bacterial metabolism of Kinneret FOM. The dramatic difference in p-comp fluorescence between the January 2009 and August 2009 samples highlights the importance of a complete year-round timecourse of FOM dynamics in future studies. It remains unclear whether autumn sampling would have revealed a drop in p-comp, bringing the component in line with January levels, or whether the Kinneret exhibits year-to-year differences in p-comp fluorescence. Future incubation studies should also gather as much microbial production data as possible in parallel with fluorescence, and researchers should consider a more sensitive measure of microbial density than direct cell counts, which did not provide sufficient precision to test for trends in this study's dataset. Overall, the continuing study of FOM in natural lake ecosystems is important. FOM studies have already begun to improve our ability to monitor productivity and lake trophic state, both in-situ and using remote sensing, and to deepen our understanding of microbial food web and limnetic recycling processes.

Conclusions

This study supported the utility of fluorescence spectrofluorometry in isolating and tracking independent fractions of the dissolved organic matter pool. Protein-like

fluorescence was identified as a potential indicator for tracking fast-paced changes in lake productivity, and the role of bacteria in producing this fluorescence signature was supported. "Marine" (autochthonous) and terrestrial humic acid fluorescence signatures were isolated, and while these signatures were coupled in situ, disparate dynamics were observed in incubation. A comparison between incubation and in situ m-comp dynamics suggested that this component may be highly dynamic, depending on sunlight exposure. A non-riverine, benthic sediment source for terrestrial humic-like fluorescence was suggested.

References

Amon, R. & R. Benner, 1996. Bacterial utilization of different size classes of dissolved organic matter. Limnology and Oceanography, 41.

Amon, R., H. Fitznar & R. Benner, 2001. Linkages among the bioreactivity, chemical composition, and diagenetic state of marine dissolved organic matter. Limnology and Oceanography, 46: 287-297.

Bahram, M., R. Bro, C. Stedmon & A. Afkhami, 2006. Handling of Rayleigh and Raman scatter for PARAFAC modeling of fluorescence data using interpolation. Journal of Chemometrics, 20: 99-105.

Baker, A. & R. G. M. Spencer, 2004. Characterization of dissolved organic matter from source to sea using fluorescence and absorbance spectroscopy. Science of The Total Environment, 333: 217-232.

Barnes, R. & K. Mann (Eds.), 1991. Fundamental of Aquatic Ecology, 2nd edition. Wiley-Blackwell.

Benner, R., 2002. Biogeochemistry of marine dissolved organic matter. *in* D. A. Hansell & C. A. Carlson (eds.) Biogeochemistry of marine dissolved organic matter. Academic Press.

Benner, R. & B. Biddanda, 1998. Photochemical Transformations of Surface and Deep Marine Dissolved Organic Matter: Effects on Bacterial Growth. Limnology and Oceanography, 43: 1373-1378.

Berman, T., B. Kaplan, S. Chava, Y. Viner, B. Sherr & E. Sherr, 2001. Metabolically active bacteria in Lake Kinneret. Aquatic Microbial Ecology, 23: 213–224.

Berman, T., A. Parparov & Y. Z. Yacobi, 2004. Lake Kinneret : Planktonic community production and respiration and the impact of bacteria on photic zone carbon cycling. Pallanza, Italy.

Berman, T., Y. Z. Yacobi, A. Parparov & G. Gal, 2010. Estimation of long-term bacterial respiration and growth efficiency in Lake Kinneret. FEMS Microbiology Ecology.

Berman, T., Y. Z. Yacobi & U. Pollingher, 1992. Lake Kinneret phytoplankton: Stability and variability during twenty years (1970?1989). Aquatic Sciences, 54: 104-127.

Berman, T. & U. Pollingher, 1974. Annual and Seasonal Variations of Phytoplankton, Chlorophyll, and Photosynthesis in Lake Kinneret. Limnology and Oceanography, 19: 31-54.

Berman, T., Y. Z. Yacobi, A. Parparov & G. Gal, 2009. Estimation of long-term bacterial respiration and growth e/ciency in Lake Kinneret. FEMS Microbiology Ecology.

Berman, T., Y. Z. Yacobi, A. Parparov & G. Gal, 2010. Estimation of long-term bacterial respiration and growth efficiency in Lake Kinneret. FEMS Microbiology Ecology, 71: 351-363.

Blough, N. V. & R. Del Vecchio, 2002. Chromophoric DOM in the Coastal Environment. Pages 509-546 *in* A. H. Dennis & A. C. Craig (eds.) Biogeochemistry of Marine Dissolved Organic Matter. Academic Press, San Diego.

Borisover, M., Y. Laor, A. Parparov, N. Bukhanovsky & M. Lado, 2009. Spatial and seasonal patterns of fluorescent organic matter in Lake Kinneret (Sea of Galilee) and its catchment basin. Water Research, 43: 3104-3116.

Cammack, W., J. Kalff, Y. Prairie & E. Smith, 2004. Fluorescent dissolved organic matter in lakes: Relationships with heterotrophic metabolism. Limnology and Oceanography, 49: 2034-2045.

Chen, R. F., P. Bissett, P. Coble, R. Conmy, G. B. Gardner, M. A. Moran, X. Wang, M. L. Wells, P. Whelan & R. G. Zepp, 2004a. Chromophoric dissolved organic matter (CDOM) source characterization in the Louisiana Bight. Marine Chemistry, 89:

257-272.
Chen, Z., Y. Li & J. Pan, 2004b. Distributions of colored dissolved organic matter and dissolved organic carbon in the Pearl River Estuary, China. Continental Shelf Research, 24: 1845-1856.
Coble, P. G., 1996. Characterization of marine and terrestrial DOM in seawater using excitation emission matrix spectroscopy. Marine Chemistry, 51: 325-346.
Coble, P. G., S. A. Green, N. V. Blough & R. B. Gagosian, 1990. Characterization of dissolved organic matter in the Black Sea by fluorescence spectroscopy. Nature, 348: 432-435.
De Souza Sierra, M., O. Donard, M. Lamotte, C. Belin & M. Ewald, 1994. Fluorescence spectroscopy of coastal and marine waters. Marine Chemistry, 47: 127-144.
Donard, O. F. X., M. Lamotte, C. Belin & M. Ewald, 1989. High-sensitivity fluorescence spectroscopy of mediterranean waters using a conventional or a pulsed laser excitation source. Marine Chemistry, 27: 117-136.
Fenchel, T., 2008. The microbial loop – 25 years later. Journal of Experimental Marine Biology and Ecology, 366: 99-103.
Ferrari, G. M. & M. D. Dowell, 1998. CDOM Absorption Characteristics with Relation to Fluorescence and Salinity in Coastal Areas of the Southern Baltic Sea. Estuarine, Coastal and Shelf Science, 47: 91-105.
Ferrari, G. & S. Tassan, 1991. On the accuracy of determining light absorption by "yellow substance" through measurements of induced fluorescence. Limnology and Oceanography, 36: 777-786.
Ferrari, G. M., 2000. The relationship between chromophoric dissolved organic matter and dissolved organic carbon in the European Atlantic coastal area and in the West Mediterranean Sea (Gulf of Lions). Marine Chemistry, 70: 339-357.
Ferrari, G. M., M. D. Dowell, S. Grossi & C. Targa1, 1996. Relationship between the optical properties of chromophoric dissolved organic matter and total concentration of dissolved organic carbon in the southern Baltic Sea region. Marine Chemistry, 55: 299-316.
Findlay, S. & R. L. Sinsabaugh, 2003. Aquatic ecosystems. Academic Press.
Gafny, S. & A. Gasith, 1993. Effect of low water level on the water quality of the littoral zone in Lake Kinneret. Water Science and Technology, 27: 363-371.
del Giorgio, P. A. & J. J. Cole, 1998. Bacterial Growth Efficiency in Natural Aquatic Systems. Annual Review of Ecology and Systematics, 29: 503-541.
Hansell, D. A. & C. A. Carlson, 2002. Biogeochemistry of Marine Dissolved Organic Matter.
Hart, D. R., L. Stone & T. Berman, 2000. Seasonal dynamics of the Lake Kinneret food web: The importance of the microbial loop. Limnology and Oceanography, 45: 350-361.
Hernes, P. J. & R. Benner, 2006. Terrigenous organic matter sources and reactivity in the North Atlantic Ocean and a comparison to the Arctic and Pacific oceans. Marine Chemistry, 100: 66-79.
Hoge, F. E., R. N. Swift, J. K. Yungel & A. Vodacek, 1993. Fluorescence of Dissolved Organic Matter: A Comparison of North Pacific and North Atlantic Oceans During April 1991.
Hudson, N., A. Baker, D. Ward, D. Reynlds, C. Brunsdon, C. Carliell-Marquet & S. Browning, 2008. Can fluorescence spectrometry be used as a surrogate for the Biochemical Oxygen Demand (BOD) test in water quality assessment? An example from South West England. Science of The Total Environment, 391: 149-158.

Kolodny, Y., A. Katz, A. Starinsky, T. Moise & E. Simon, 1999. Chemical Tracing of Salinity Sources in Lake Kinneret (Sea of Galilee), Israel. Limnology and Oceanography, 44: 1035-1044.

Kowalczuk, P., W. J. Cooper, R. F. Whitehead, M. J. Durako & W. Sheldon, 2003. Characterization of CDOM in an organic-rich river and surrounding coastal ocean in the South Atlantic Bight. Aquatic Sciences - Research Across Boundaries, 65: 384-401.

Kowalczuk, P., M. J. Durako, H. Young, Am, A. E. Kahn, W. J. Cooper & M. Gonsior, 2009. Characterization of dissolved organic matter fluorescence in the South Atlantic Bight with use of PARAFAC model: Interannual variability. Marine Chemistry, 113: 182-196.

LeFèvre, J., L. Legendre & R. Rivkin, 1998. Fluxes of biogenic carbon in the Southern Ocean: roles of large microphagous zooplankton. Journal of Marine Systems, 17: 325–345.

Maji, S., K. Sundararajan & K. S. Viswanathan, 2000. Correction for quenching in fluorimetric determinations using steady state fluorescence. Spectrochimica ACTA part A-Molecular and Biomolecular Spectroscopy, 56: 1251-1256.

Markel, D., 2008. Monitoring and Managing Lake Kinneret and its Watershed, Northern Israel, a Response to Environmental, Anthropogenic and Political Constraints. *in* Watershed Management: Case Studies. ICFAI University Press.

Miller, W. L., 1999. An Overview of Aquatic Photochemistry as it Relates to Microbial Production. *in* C. R. Bell, M. Brylinsky, & P. Johnson-Green (eds.). Halifax, Canada.

Mopper, K. & E. Degens, 1979. Organic Carbon in the Ocean: Nature and Cycling. Page 293–316 *in* B. Bolin, E. Degens, S. Kempe, & P. Ketner (eds.) The Global Carbon Cycle. Wiley, New York, NY.

Mopper, K., X. Zhou, R. J. Kieber, D. J. Kieber, R. J. Sikorski & R. D. Jones, 1991. Photochemical degradation of dissolved organic carbon and its impact on the oceanic carbon cycle. Nature, 353: 60-62.

Moran, M. A. & R. G. Zepp, 1997. Role of photoreactions in the formation of biologically labile compounds from dissolved organic matter. Limnology and Oceanography, 42: 1307-1316.

Morris, D. P. & B. R. Hargreaves, 1997. The role of photochemical degradation of dissolved organic carbon in regulating the UV transparency of three lakes on the Pocono Plateau. Limnology and Oceanography, 42: 239-249.

Murphy, K. R., C. A. Stedmon, T. D. Waite & G. M. Ruiz, 2008. Distinguishing between terrestrial and autochthonous organic matter sources in marine environments using fluorescence spectroscopy. Marine Chemistry, 108: 40-58.

Nelson, N. B., C. A. Carlson & D. K. Steinberg, 2004a. Production of chromophoric dissolved organic matter by Sargasso Sea microbes. Marine Chemistry, 89: 273-287.

Nelson, N. B., C. A. Carlson & D. K. Steinberg, 2004b. Production of chromophoric dissolved organic matter by Sargasso Sea microbes. Marine Chemistry, 89: 273-287.

Nieto-Cid, M., X. A. Alvarez-Salgado & F. F. Perez, 2006. Microbial and photochemical reactivity of fluorescent dissolved organic matter in a coastal upwelling system. Limnology and Oceanography, 51: 1391-1400.

Ochiai, M., T. Nakajima & T. Hanya, 1980. Chemical composition of labile fractions in DOM. Hydrobiologia, 71: 95-97.

Ogawa, H., Y. Amagai, I. Koike, K. Kaiser & R. Benner, 2001. Production of Refractory

Dissolved Organic Matter by Bacteria. Science, 292: 917-920.
Ostapenia, A., A. Parparov & T. Berman, 2009. Lability of organic carbon in lakes of different trophic status. Freshwater Biology, 54: 1312-1323.
Pérez, M. T. & R. Sommaruga, 2007. Interactive effects of solar radiation and dissolved organic matter on bacterial activity and community structure. Environmental Microbiology, 9: 2200-2210.
Pitta, P., N. Stambler, T. Tanaka, T. Zohary, A. Tselepides & F. Rassoulzadegan, 2005. Topical Studies in Oceanography : Biological response to P addition in the Eastern Mediterranean Sea. The microbial race against time. Deep Sea Research Part II, 52: 2961-2974.
Pollingher, U., 1981. The structure and dynamics of the phytoplankton assemblages in Lake Kinneret, Israel. J. Plankton Res., 3: 93-105.
Pomeroy, L., P. J. Williams, F. Azam & J. Hobbie, 2007. The microbial loop. Oceanography, 20: 28-33.
Pomeroy, L. & W. Wiebe, 1988. Energetics of microbial food webs. Hydrobiologia, 159: 7-18.
Porter, K. & Y. Feig, 1980. The use of DAPI for identifying and counting aquatic microflora. Limnology and Oceanography, 25: 943-948.
Rimmer, A. & G. Gal, 2003. Estimating the saline springs component in the solute and water balance of Lake Kinneret, Israel. Journal of Hydrology, 284: 228-243.
Rochelle-Newall, E. J. & T. R. Fisher, 2002. Production of chromophoric dissolved organic matter fluorescence in marine and estuarine environments: an investigation into the role of phytoplankton. Marine Chemistry, 77: 7-21.
Rosenstock, B., W. Zwisler & M. Simon, 2005. Bacterial Consumption of Humic and Non-Humic Low and High Molecular Weight DOM and the Effect of Solar Irradiation on the Turnover of Labile DOM in the Southern Ocean. Microbial Ecology, 50: 90-101.
Siegel, D. A., S. Maritorena, N. B. Nelson, D. A. Hansell & M. Lorenzi-Kayser, 2002. Global distribution and dynamics of colored dissolved and detrital organic materials. Journal of Geophysical Research-Oceans, 107.
Simon, M. & F. Azam, 1989. Protein content and protein synthesis rates of planktonic marine bacteria. Marine Ecology-Progress Series, 51: 201-213.
Smith, E. & R. Benner, 2005. Photochemical transformations of riverine dissolved organic matter: effects on estuarine bacterial metabolism and nutrient demand. Aquatic Microbial Ecology, 40: 37-50.
Stedmon C.A., Markager S. & Bro R., 2003. Tracing dissolved organic matter in aquatic environments using a new approach to fluorescence spectroscopy. Marine Chemistry, 82: 239-254.
Stedmon, C. A. & R. Bro, 2008. Characterizing dissolved organic matter fluorescence with paral- lel factor analysis: a tutorial. Limnology and Oceanography: Methods, 6: 572-579.
Stedmon, C. A., S. Markager & R. Bro, 2003. Tracing dissolved organic matter in aquatic environments using a new approach to fluorescence spectroscopy. Marine Chemistry, 82: 239-254.
Stedmon, C. A. & S. Markager, 2005a. Resolving the variability in dissolved organic matter fluorescence in a temperate estuary and its catchment using PARAFAC analysis. Limnology and Oceanography, 50: 686-697.
Stedmon, C. & S. Markager, 2005b. Tracing the production and degradation of autochthonous fractions of dissolved organic matter by fluorescence analysis. Limnology and Oceanography, 50: 1415-1426.

Tedetti, M. & R. Sempere, 2006. Penetration of ultraviolet radiation in the marine environment. A review. Photochemistry and Photobiology, 82: 389-397.
Tranvik, L. J. [. & S. [. Bertilsson, 2001. Contrasting effects of solar UV radiation on dissolved organic sources for bacterial growth. Ecology Letters, 4: 458-463.
Tyler, J. E., 1968. The Secchi Disc. Limnology and Oceanography, 13: 1-6.
Udenfriend, S., 1962. Fluorescence Assay in Biology and Medicine. Academic Press, New York, NY.
Vodacek, A., N. V. Blough, M. D. DeGrandpre, E. T. Peltzer & R. K. Nelson, 1997. Seasonal variation of CDOM and DOC in the Middle Atlantic Bight: Terrestrial inputs and photooxidation. Limnology and Oceanography, 42: 674-686.
Weiss, M. & M. Simon, 1999. Consumption of labile dissolved organic matter by limnetic bacterioplankton: the relative significance of amino acids and carbohydrates. Aquatic Microbial Ecology, 17: 1-12.
Zhao, J., W. Cao, G. Wang, D. Yang, Y. Yang, Z. Sun, W. Zhou & S. Liang, 2009. The variations in optical properties of CDOM throughout an algal bloom event. Estuarine, Coastal and Shelf Science, 82: 225-232.
Zohary, T., 2004. Changes to the phytoplankton assemblage of Lake Kinneret after decades of a predictable, repetitive pattern. Freshwater Biology, 49: 1355-1371.

Appendix: Flow of data analysis.

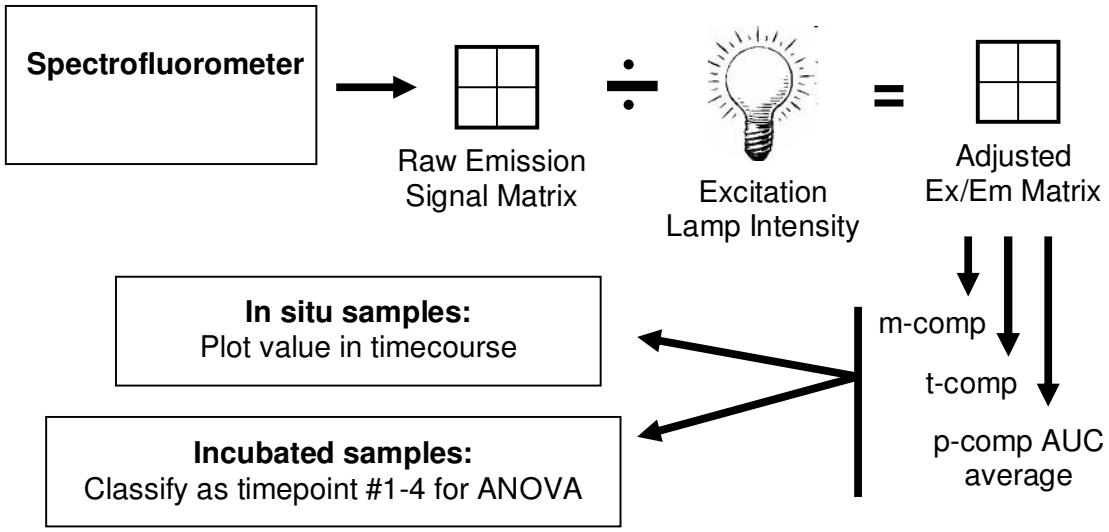

Raw emission count matrix

Excitation (across) / Emission (down)	260	270	280	290	300	310	320	330	340	350	360
290	930	840	1140	1.2E+05	1050	610	530	550	640	490	540
294	570	2330	990	4.6E+04	5970	570	640	490	530	510	460
298	620	4350	1420	2380	1.47E+05	530	340	540	470	520	540
302	730	2250	1940	1350	1.47E+05	2740	510	540	670	520	500
306	710	1260	4870	1630	1.3E+04	8.4E+04	560	520	470	500	640
310	860	1650	8480	2330	1770	3.2E+05	1060	540	550	510	430
314	1100	1980	5260	3260	1110	1.1E+05	9450	630	570	490	480
318	960	2370	4000	8480	1560	3900	3.5E+05	470	490	410	610
322	1260	2460	4110	1.4E+04	1870	680	4.1E+05	5390	560	610	710
326	1320	2600	4970	8680	2030	1070	3.5E+04	1.9E+05	510	390	490
330	1220	2840	5540	5810	7360	1130	2690	7.3E+05	1690	590	600
334	1280	3080	6430	5530	1.6E+04	1600	980	3.1E+05	1.7E+04	540	580
338	1720	3310	6600	6410	9690	1630	1430	9210	7.0E+05	530	580
342	1370	3140	6190	6830	3680	6390	1500	1440	8.8E+05	6260	730
346	1850	3660	6740	7290	3700	1.7E+04	1750	1370	8.7E+04	2.5E+05	500
350	2020	4030	6910	6960	3850	1.3E+04	2360	1730	4750	1.1E+06	1390
354	1810	4080	7140	7730	3990	5290	6510	2410	1800	5.0E+05	1.7E+04
358	1510	3950	6750	7920	4760	4050	2.1E+04	2920	2180	1.1E+04	9.0E+05
362	2050	4080	7000	8280	5360	4600	2.0E+04	4020	2520	2140	1.3E+06
366	1970	4370	6920	7970	5380	4940	8280	7480	2850	1970	1.4E+05
370	1970	4000	6530	7930	6060	5780	5970	2.1E+04	4010	2500	6060
374	2170	4170	7190	7430	6320	5630	6580	2.5E+04	4730	2630	2010
378	2220	3430	6770	8440	6560	7300	6580	1.2E+04	7950	3450	2260
382	2180	4400	6520	7570	7180	7670	7620	7760	2.0E+04	4350	2880
386	2320	4030	6760	7550	7640	8500	7800	8240	2.7E+04	4730	3540
390	2340	3910	6120	8310	8460	7940	8610	8630	1.6E+04	7400	3820
394	2040	3550	6230	7620	7140	8010	8400	9040	9160	1.7E+04	4330
398	2110	3690	5860	7510	8160	7870	9060	8540	7900	2.6E+04	4590
402	2340	3530	5350	7100	7740	7550	8680	8700	8280	1.7E+04	6130
406	2400	3560	5550	6900	7570	8180	8240	9650	8540	8350	1.2E+04
410	2170	3690	5030	6420	7070	8110	8130	9090	8600	8050	2.1E+04
414	2180	4040	5160	6380	7760	8220	8690	9080	8280	7820	1.9E+04
418	2740	3670	4760	6610	6830	7980	8770	8690	9040	8450	1.0E+04
422	2510	3900	5450	6520	7510	7470	8850	9270	8930	8640	8400
426	2540	3960	5280	6550	6800	7730	8320	9400	9940	9130	8650
430	2500	3920	5370	6170	7160	7860	8610	9220	9450	9090	8500
434	2340	3820	5870	6290	6620	6800	8640	9070	9300	9130	8090
438	2720	3880	4780	6520	6370	6870	8270	9450	9610	9840	8990
442	2800	3910	5290	6520	6440	6640	7490	8350	9630	9430	8980
446	2510	4020	5160	5610	6270	6850	7830	9060	1.0E+04	9510	8980
450	2390	4270	5340	5910	6680	7490	7650	8770	9320	9270	9330
454	2840	3920	5230	5910	6160	6220	7580	8120	8740	9050	9160
458	2510	4110	4820	5570	5810	6210	6650	7750	8460	9320	9070
462	2190	3870	4800	5330	5330	6410	6520	8390	8220	8510	8330

divided by
Spectrofluorometer lamp intensity:

Excitation (across)	260	270	280	290	300	310	320	330	340	350	360
Emission (down)											
290	**0.004**	**0.008**	**0.013**	**0.020**	**0.025**	**0.028**	**0.033**	**0.039**	**0.045**	**0.049**	**0.051**
294	0.004	0.008	0.013	0.020	0.025	0.028	0.033	0.039	0.045	0.049	0.051
298	0.004	0.008	0.013	0.020	0.025	0.028	0.033	0.039	0.045	0.049	0.051
302	0.004	0.008	0.013	0.020	0.025	0.028	0.033	0.039	0.045	0.049	0.051
306	0.004	0.008	0.013	0.020	0.025	0.028	0.033	0.039	0.045	0.049	0.051
310	0.004	0.008	0.013	0.020	0.025	0.028	0.033	0.039	0.045	0.049	0.051
314	0.004	0.008	0.013	0.020	0.025	0.028	0.033	0.039	0.045	0.049	0.051
318	0.004	0.008	0.013	0.020	0.025	0.028	0.033	0.039	0.045	0.049	0.051
322	0.004	0.008	0.013	0.020	0.025	0.028	0.033	0.039	0.045	0.049	0.051
326	0.004	0.008	0.013	0.020	0.025	0.028	0.033	0.039	0.045	0.049	0.051
330	0.004	0.008	0.013	0.020	0.025	0.028	0.033	0.039	0.045	0.049	0.051
334	0.004	0.008	0.013	0.020	0.025	0.028	0.033	0.039	0.045	0.049	0.051
338	0.004	0.008	0.013	0.020	0.025	0.028	0.033	0.039	0.045	0.049	0.051
342	0.004	0.008	0.013	0.020	0.025	0.028	0.033	0.039	0.045	0.049	0.051
346	0.004	0.008	0.013	0.020	0.025	0.028	0.033	0.039	0.045	0.049	0.051
350	0.004	0.008	0.013	0.020	0.025	0.028	0.033	0.039	0.045	0.049	0.051
354	0.004	0.008	0.013	0.020	0.025	0.028	0.033	0.039	0.045	0.049	0.051
358	0.004	0.008	0.013	0.020	0.025	0.028	0.033	0.039	0.045	0.049	0.051
362	0.004	0.008	0.013	0.020	0.025	0.028	0.033	0.039	0.045	0.049	0.051
366	0.004	0.008	0.013	0.020	0.025	0.028	0.033	0.039	0.045	0.049	0.051
370	0.004	0.008	0.013	0.020	0.025	0.028	0.033	0.039	0.045	0.049	0.051
374	0.004	0.008	0.013	0.020	0.025	0.028	0.033	0.039	0.045	0.049	0.051
378	0.004	0.008	0.013	0.020	0.025	0.028	0.033	0.039	0.045	0.049	0.051
382	0.004	0.008	0.013	0.020	0.025	0.028	0.033	0.039	0.045	0.049	0.051
386	0.004	0.008	0.013	0.020	0.025	0.028	0.033	0.039	0.045	0.049	0.051
390	0.004	0.008	0.013	0.020	0.025	0.028	0.033	0.039	0.045	0.049	0.051
394	0.004	0.008	0.013	0.020	0.025	0.028	0.033	0.039	0.045	0.049	0.051
398	0.004	0.008	0.013	0.020	0.025	0.028	0.033	0.039	0.045	0.049	0.051
402	0.004	0.008	0.013	0.020	0.025	0.028	0.033	0.039	0.045	0.049	0.051
406	0.004	0.008	0.013	0.020	0.025	0.028	0.033	0.039	0.045	0.049	0.051
410	0.004	0.008	0.013	0.020	0.025	0.028	0.033	0.039	0.045	0.049	0.051
414	0.004	0.008	0.013	0.020	0.025	0.028	0.033	0.039	0.045	0.049	0.051
418	0.004	0.008	0.013	0.020	0.025	0.028	0.033	0.039	0.045	0.049	0.051
422	0.004	0.008	0.013	0.020	0.025	0.028	0.033	0.039	0.045	0.049	0.051
426	0.004	0.008	0.013	0.020	0.025	0.028	0.033	0.039	0.045	0.049	0.051
430	0.004	0.008	0.013	0.020	0.025	0.028	0.033	0.039	0.045	0.049	0.051
434	0.004	0.008	0.013	0.020	0.025	0.028	0.033	0.039	0.045	0.049	0.051
438	0.004	0.008	0.013	0.020	0.025	0.028	0.033	0.039	0.045	0.049	0.051
442	0.004	0.008	0.013	0.020	0.025	0.028	0.033	0.039	0.045	0.049	0.051
446	0.004	0.008	0.013	0.020	0.025	0.028	0.033	0.039	0.045	0.049	0.051
450	0.004	0.008	0.013	0.020	0.025	0.028	0.033	0.039	0.045	0.049	0.051
454	0.004	0.008	0.013	0.020	0.025	0.028	0.033	0.039	0.045	0.049	0.051
458	0.004	0.008	0.013	0.020	0.025	0.028	0.033	0.039	0.045	0.049	0.051
462	0.004	0.008	0.013	0.020	0.025	0.028	0.033	0.039	0.045	0.049	0.051

=

Adjusted excitation/emission signal matrix:

Excitation (across) / Emission (down)	260	270	280	290	300	310	320	330	340	350	360
290	2.15E+05	1.01E+05	8.45E+04	6.15E+06	4.24E+04	2.18E+04	1.62E+04	1.42E+04	1.44E+04	9937.939	1.05E+04
294	1.32E+05	2.80E+05	7.39E+04	2.27E+06	2.41E+05	2.03E+04	1.95E+04	1.27E+04	1.19E+04	1.03E+04	8967.386
298	1.44E+05	5.24E+05	1.06E+05	1.19E+05	5.96E+06	1.89E+04	1.04E+04	1.40E+04	1.05E+04	1.05E+04	1.05E+04
302	1.70E+05	2.70E+05	1.43E+05	6.73E+04	5.94E+06	9.83E+04	1.56E+04	1.40E+04	1.50E+04	1.05E+04	9707.041
306	1.65E+05	1.51E+05	3.61E+05	8.13E+04	5.33E+05	3.01E+06	1.72E+04	1.34E+04	1.05E+04	1.01E+04	1.25E+04
310	2.00E+05	1.99E+05	6.31E+05	1.16E+05	7.12E+04	1.13E+07	3.24E+04	1.40E+04	1.23E+04	1.04E+04	8364.945
314	2.56E+05	2.38E+05	3.91E+05	1.62E+05	4.47E+04	3.99E+06	2.88E+05	1.62E+04	1.28E+04	9957.326	9290.622
318	2.22E+05	2.85E+05	2.97E+05	4.26E+05	6.30E+04	1.39E+05	1.07E+07	1.22E+04	1.10E+04	8292.042	1.18E+04
322	2.93E+05	2.97E+05	3.05E+05	1.16E+05	7.53E+04	2.43E+04	1.26E+07	1.39E+05	1.25E+04	1.24E+04	1.38E+04
326	3.07E+05	3.13E+05	3.70E+05	4.34E+05	8.18E+04	3.82E+04	1.07E+06	4.96E+06	1.14E+04	7900.494	9521.219
330	2.84E+05	3.42E+05	4.11E+05	2.90E+05	2.98E+05	4.04E+04	8.20E+04	1.87E+07	3.80E+04	1.19E+04	1.16E+04
334	2.97E+05	3.72E+05	4.77E+05	2.76E+05	6.23E+05	5.71E+04	3.00E+04	7.89E+06	3.88E+05	1.09E+04	1.13E+04
338	4.03E+05	3.99E+05	4.89E+05	3.21E+05	3.89E+05	5.80E+04	4.37E+04	2.39E+05	1.57E+07	1.07E+04	1.12E+04
342	3.18E+05	3.79E+05	4.61E+05	3.41E+05	1.48E+05	2.28E+05			1.96E+07	1.27E+05	1.42E+04
346	4.30E+05	4.42E+05	5.00E+05	3.64E+05	1.49E+05	6.16E+05			1.94E+06	5.10E+06	9691.801
350	4.70E+05	4.88E+05	5.13E+05	3.47E+05	1.55E+05	4.72E+05			1.06E+05	2.31E+07	2.69E+04
354	4.21E+05	4.93E+05	5.31E+05	3.87E+05	1.61E+05	1.89E+05	2.00E+05	6.23E+04	4.01E+04	1.02E+07	3.33E+05
358	3.51E+05	4.77E+05	5.02E+05	3.95E+05	1.92E+05	1.45E+05	6.44E+05	7.56E+04	4.88E+04	2.28E+05	1.74E+07
362	4.77E+05	4.92E+05	5.22E+05	4.12E+05	2.15E+05	1.64E+05	6.01E+05	1.04E+05	5.62E+04	4.32E+04	2.45E+07
366	4.59E+05	5.26E+05	5.14E+05	3.97E+05	2.17E+05	1.76E+05	2.53E+05	1.94E+05	6.36E+04	4.00E+04	2.68E+06
370	4.58E+05	4.83E+05	4.86E+05	3.95E+05	2.44E+05	2.06E+05	1.83E+05	5.42E+05	8.95E+04	5.07E+04	1.17E+05
374	5.06E+05	5.02E+05	5.32E+05	3.72E+05	2.55E+05	2.01E+05	2.01E+05	6.46E+05	1.06E+05	5.33E+04	3.90E+04
378	5.16E+05	4.13E+05	5.02E+05	4.21E+05	2.64E+05	2.61E+05	2.01E+05	3.04E+05	1.78E+05	6.99E+04	4.37E+04
382	5.08E+05	5.30E+05	4.86E+05	3.77E+05	2.90E+05	2.73E+05	2.34E+05	2.01E+05	4.39E+05	8.80E+04	5.58E+04
386	5.40E+05	4.86E+05	5.04E+05	3.76E+05	3.09E+05	3.04E+05	2.39E+05	2.13E+05	6.08E+05	9.60E+04	6.88E+04
390	5.45E+05	4.70E+05	4.55E+05	4.15E+05	3.41E+05	2.85E+05	2.63E+05	2.23E+05	3.48E+05	1.50E+05	7.42E+04
394	4.75E+05	4.27E+05	4.63E+05	3.80E+05	2.88E+05	2.86E+05	2.58E+05	2.34E+05	2.06E+05	3.37E+05	8.41E+04
398	4.90E+05	4.43E+05	4.36E+05	3.74E+05	3.27E+05	2.82E+05	2.77E+05	2.20E+05	1.76E+05	5.29E+05	8.92E+04
402	5.44E+05	4.26E+05	3.97E+05	3.53E+05	3.12E+05	2.93E+05	2.72E+05	2.24E+05	1.86E+05	3.54E+05	1.19E+05
406	5.57E+05	4.29E+05	4.12E+05	3.43E+05	3.04E+05	2.93E+05	2.52E+05	2.49E+05	1.91E+05	1.69E+05	2.39E+05
410	5.04E+05	4.48E+05	3.74E+05	3.20E+05	2.85E+05	2.89E+05	2.49E+05	2.35E+05	1.93E+05	1.63E+05	4.15E+05
414	5.07E+05	4.90E+05	3.82E+05	3.18E+05	3.13E+05	2.94E+05	2.66E+05	2.35E+05	1.85E+05	1.59E+05	3.62E+05
418	6.38E+05	4.41E+05	3.53E+05	3.31E+05	2.75E+05	2.85E+05	2.68E+05	2.24E+05	2.02E+05	1.72E+05	2.01E+05
422	5.86E+05	4.72E+05	4.04E+05	3.26E+05	3.02E+05	2.67E+05	2.71E+05	2.39E+05	2.00E+05	1.75E+05	1.63E+05
426	5.92E+05	4.77E+05	3.93E+05	3.28E+05	2.75E+05	2.76E+05	2.54E+05	2.44E+05	2.22E+05	1.85E+05	1.68E+05
430	5.82E+05	4.73E+05	3.99E+05	3.07E+05	2.89E+05	2.81E+05	2.64E+05	2.38E+05	2.12E+05	1.84E+05	1.64E+05
434	5.44E+05	4.59E+05	4.37E+05	3.14E+05	2.67E+05	2.43E+05	2.63E+05	2.36E+05	2.08E+05	1.86E+05	1.57E+05
438	6.34E+05	4.68E+05	3.56E+05	3.25E+05	2.58E+05	2.45E+05	2.54E+05	2.45E+05	2.15E+05	2.00E+05	1.74E+05
442	6.51E+05	4.71E+05	3.94E+05	3.26E+05	2.59E+05	2.38E+05	2.29E+05	2.16E+05	2.15E+05	1.91E+05	1.74E+05
446	5.83E+05	4.86E+05	3.83E+05	2.80E+05	2.52E+05	2.44E+05	2.40E+05	2.34E+05	2.24E+05	1.93E+05	1.74E+05
450	5.55E+05	5.15E+05	3.99E+05	2.95E+05	2.71E+05	2.68E+05	2.35E+05	2.27E+05	2.09E+05	1.83E+05	1.78E+05
454	6.61E+05	4.71E+05	3.87E+05	2.95E+05	2.48E+05	2.22E+05	2.31E+05	2.10E+05	1.96E+05	1.83E+05	1.78E+05
458	5.81E+05	4.94E+05	3.58E+05	2.77E+05	2.34E+05	2.22E+05	2.04E+05	2.01E+05	1.89E+05	1.89E+05	1.76E+05
462	5.11E+05	4.68E+05	3.57E+05	2.66E+05	2.15E+05	2.29E+05	2.00E+05	2.17E+05	1.84E+05	1.73E+05	1.62E+05

Sum / 16 = p-comp AUC

m-comp

t-comp

Hebrew Supplement:

תקציר

זרימת אנרגיה וביומאסה דרך שרשרת המזון בסביבה המימית נובעת מתהליכי פוטוסינתזה, רעייה וטריפה וכן כתוצאה מצריכה של חומר אורגאני מומס וחלקיקי ע"י חיידקים. ביומאסה בקטריאלית נכנסת למארג המזון דרך המחזור המיקרוביאלי (microbial loop). במחזור זה חיידקים נאכלים על ידי מיקרוזואופלנקטון מקבוצות הריסניות והננופלאגלטים. קבוצות אלו משמשות כטרף לזואופלנקטון גדול יותר וכך מועברת הביומאסה המיקרוביאלית במעלה מארג המזון. במערכות כמו אגם הכנרת, המחזור המיקרוביאלי עשוי לייצג את מעברי האנרגיה הגדולים ביותר במארג המזון. יחד עם זאת, אופי המעברים הספציפיים של חומר אורגאני בעמודת המים עדיין אינו מובן לחלוטין, כך גם האינטראקציות בין חומר אורגאני מומס בעל צבע לבין האוכלוסייה המיקרוביאלית. חומר אורגאני מומס כרומופורי (CDOM = חואמ"כ) הינו תערובת המורכבת מחומצות אמיניות, חלבונים, חומצות הומיות (humic acids) וסוכרים אשר קולטת אור. חואמ"כ משפיע על מספר פרמטרים במערכת האקולוגית הכוללים: זמינות אור, צריכת חמצן ביולוגית (BOD), מיקרו-נוטריאנטים וריכוזי חמצן פעיל. מקור החואמ"כ יכול להיות יבשתי (המסת קרקע) או ביולוגי. דבר המשפיע על הרכבו הכימי ונטייתו להגיב כימית וכתוצאה מכך גם על פעילותו האופטית. כאשר חואמ"כ מיוצר ביולוגית בעמודת המים (כתוצר לוואי של פעילות אצות, חיידקים ובעלי חיים), הוא מורכב מחלבונים וחומצות הומיות 'ימיות'. בתהליכים פוטו-ראקטיבים החואמ"כ מפורק למרכיבים בעלי משקל מולקולרי קטן יותר, העשויים להשפיע על יכולתו לשמש מצע גידול מיקרוביאלי. עקב השונות הגדולה בהרכב החואמ"כ קשה לכמת את מידת זמינותו לצריכת חיידקים. למרות זאת, כלים חדשים לכימות ואפיון חואמ"כ במערכות טבעיות פותחו לאחרונה וביניהם בולט ניתוח ספקטרופלואורומטרי של המרכיב הפלואורסנטי של חואמ"כ. שיטה זו מאפשרת להפריד ולכמת את הפלואורסנציה של חלקים מוגדרים מתוך כלל המאגר של החואמ"כ בהתאם לשיאי הערור/פליטה האופטיים שלהם. מחקר זה מוסיף על מחקרו של בוריסובר וחובריו (2009) שבו זוהו שלושה רכיבים פלואורסצנטיים עיקריים הכוללים: שיא אחד בטווח הפלואורוסנטי של טריפטופאן (מרכיב P- דמוי חלבון), שיא אחד בטווח של חומצות הומיות שמקורן בקרקעות יבשתיות (מרכיב T) ומרכיב אחד שזוהה במחקרים קודמים כמצטבר בעמודת המים (מרכיב M- דמוי חומצות הומיות 'ימיות'). מחקרי משתמש בניתוח ספקטרופלואורומטרי על מנת לחקור מגמות עונתיות בפלואורסנציה של חואמ"כ באגם הכנרת ומנסה לקשר את הדינאמיקה של חואמ"כ פלואורסצנטי לתהליכי פירוק מיקרוביאלי של ביומאסה הנוצרת על ידי אצות באגם. השערת המחקר היתה שפירוק מיקרוביאלי של חומר אורגני מומס וחלקיקי שמקורו בפריחת האצות, קובע את ריכוזי החואמ"כ הפלורוסנטי דמוי החלבון בכנרת. בנוסף ציפינו למצוא הצטברות של מרכיבים אלו באינקובציה כתוצרי פירוק חומר אורגאני מומס ולקשור בין כניסת מי הירדן לבין המקור היבשתי של חואמ"כ פלואורסצנטי. לצורך בדיקת ההשערות נלקחו דגימות מעומק של 1 מטר בתחנה A, המשמשת כאתר לניטור ארוך טווח על ידי המעבדה לחקר הכנרת. הדגימות לא נחשפו לאור שמש לפני האנליזה על מנת למנוע פירוק של החואמ"כ על ידי קרינה. על מנת לייצר מטריצות ערור/פליטה נעשה שימוש בספקטרופלואורמטריה. שיא

ערור/פליטה של הרכיבים הפלואורסנטים העיקריים בודדו מהמטריצות בשיטת "Parallel Factor Analysis " שנערכה בכנרת על ידי בוריסובר וחובריו ב- 2009. לאור מיקום שיאי הפלואורסנציה במרכיבים אלו בכנרת, לא היה צורך לבצע תיקוני פיזור אופטי בנתונים אלה. המחקר עקב אחרי שלושה מרכיבים מרכזיים אלו של מאגר החומר האורגאני הפלואורסנטי בשכבת הערבוב העליונה של האגם לאורך שבעה חודשים. על מנת לזהות השפעות של פריחת אצות על דינאמיקת החואמ"כ הפלואורסנטי, הוגברה תדירות הדגימה בתקופת החורף, המתאפיינת ביצרנות מוגברת. מים משכבת הערבוב העליונה באגם (ללא תוספות) נלקחו אחת לחודש במשך ארבעה חודשים, עברו אינקובציה במעבדה ושימשו למעקב אחר השפעת הפירוק המיקרוביאלי על החומר האורגני הפלואורסנטי. המים אוחסנו בבקבוקי זכוכית אטומים בחושך, בטמפרטורה של $20^{o}C$ ומבלי שיגיעו למצב שהחמצן מהווה גורם מגביל לחיידקים המפרקים. במהלך כשלושה שבועות נלקחו ארבע עד שש דגימות מכל אחת מארבע האינקובציות. דגימות אלו עברו אנליזה ספקטרופוטומטרית וכימות של היצרנות המיקרוביאלית על ידי בדיקת קצב צריכת הלאוצין. ספירת תאים בקטריאלים נעשתה על ידי מיקרוסקופיה אפיפלורסצנטית, אך הספירה לא הניבה הבדלים משמעותיים. מעקב עונתי שנערך באגם הראה כי בחורף, במהלך תקופת היצרנות, החומר האורגאני הפלואורסנטי על פני השטח אופיין על ידי מרכיב P דינאמי (שיא ערור/פליטה ב-280/322-382 ננומטר) המשתנה בעד 14% לשבוע ומרכיבים T (שיא ערור/פליטה ב- 360/458) ו-M (שיא ערור/פליטה ב- 310/394) בעלי סיגנל חלש ויציב יותר המוגדרים כ'יבשתי' ו'ימי' בהתאמה. עוצמת האות של מרכיב ה-P עלתה וירדה באופן משמעותי שלוש פעמים ברצף בין ינואר לאפריל. יצרנות בקטריאלית של מרכיב ה-P נמצאה כגבוהה ביותר בחודש אפריל הן באגם והן באינקובציה. באופן דומה, גם הצטברות מרכיב ה-M באינקובציה נמצאה הגבוהה ביותר בחודש זה. נמצא קשר ליניארי בין מרכיב ה-T ומרכיב ה-M מתחילת שיכוב האגם ועד לסוף הקיץ. לאחר התייצבות השיכוב נמצאה ירידה הדרגתית בכל שלושת המרכיבים. כמו כן, נמצא קשר ליניארי בין מרכיב ה-P לביומאסת הפיטופלנקטון, ריכוז כלורופיל a ועומקי סקי (Secchi) שנמדדו באתר, כאשר הקשר נמצא כחזק יותר כאשר הפרמטרים נמדדו ברזולוציה גבוהה. תוצאה זו מראה כי בכדי לזהות את כל שיאי הייצור של מרכיב ה-P בתקופת היצרנות החורפית, יש להשתמש בדגימות תכופות יותר. מדידות אינקובציות מוחשכות של דגימות מי אגם בעלי ריכוזי חואמ"כ טבעיים הראו יצרנות של מרכיבי P ו-M. חומר חלקיקי היה מקור של עד 91% מן הייצור של מרכיב-M, עד 73% מן הייצור של מרכיב-P, ועד 52% מייצור הפחמן המיקרוביאלי. על פי תוצאות אלו ניתן לשער כי המרכיב החלקיקי הינו מקור חואמ"כ פלואורסצנטי חשוב וזמין יותר מששוער עד כה. תוצאות אלו סותרות מחקרים קודמים שהראו שלסינון ישנה השפעה מזערית על האות הפלורוסנטי של מי האגם. ריכוזי מרכיב ה-T לא השתנו בצורה מובהקת באינקובציה. תוצאה זו מעידה על כך שמרכיב זה אינו מצע או תוצר של יצרנות מיקרוביאלית בעמודת המים ותומכת בזיהוי של מקור יבשתי למרכיב זה. לעומת זאת, ריכוזי מרכיב ה-T לא נמצאו כקשורים לכניסה של נגר עונתי מנהר הירדן. תוצאה המעידה על מקור סדימנטרי של מרכיב זה בכנרת. היצרנות המוגברת של חומר אורגאני פלורוסנטי באינקובציה משקפת בצורה טובה את הגידול עונתי ביצרנות הפיטופלנקטון ויצרנות החיידקים. מחקר זה מעיד על קשר בין פירוק מיקרוביאלי של ביומאסת אצות לבין יצור של חומר אורגאני פלורוסנטי דמוי חומצות הומיות ודמוי חלבון. החוסר בהצטברות מרכיב ה-M במי

האגם, למרות ההצטברות שלו באינקובציות מוחשכות, תומך בכך שהלבנה על ידי אור (photobleaching) מווסתת מרכיב זה. מחקר זה מראה את היכולת של מרכיב ה-P לעקוב אחר הדינאמיקה העונתית של אוכלוסיית האצות, למרות שקשר זה נמצא כתלוי בתדירות הדגימה. קצב הייצור והפירוק של המרכיב הפלואורסנטי דמוי החלבון באגם נמצא כמהיר יותר מהקצב שדווח במחקרים עונתיים אחרים. ממצא זה מצביע על כך שקצב השינוי המרבי במרכיב זה טרם זוהה. אני מציע שפלואורוסנצית מרכיב ה-P דמוי החלבון עשויה לשמש למדד חלופי ליצרנות ראשונית בכנרת ובמערכות אקווטיות אחרות, וממליץ לחקור את האפשרות לשימוש במרכיב זה כמדד זול, רגיש ומהיר ליצרנות. קיים גם צורך במחקר נוסף שיבהיר את תפקיד ההלבנה (photobleaching) ברגולצית הפלואורוסנציה של המרכיב ה'ימי', דמוי החומצות ההומיות בכינרת.

תודות

ברצוני להודות לדר' ארקאדי פרפרוב ולתומס ברמן ממעבדת חקר הכנרת על תמיכתם החומרית והמקצועית, ולפרופסורים תמר זוהרי ויוסי יעקבי על שהעניקו לי בנדיבותם גישה לנתוני כלורופיל וביומסה של פיטופלנקטון ממחקרם. תודות גם לפרופסור מיכאל בוריסובר על הערותיו החשובות במהלך שלב התכנון של המחקר ולפרופסור יואב לבני מהטכניון על השימוש בספקטרופלאורומטר. מקרב לב אודה גם לצוות הטכנאים המקצועי והאדיב של מעבדת חקר הכנרת ובמיוחד למוטי דיאמונד ומאיר אריאלי. מחקר זה נעשה בהנחייתו של פרופ' יוחאי כרמל מהפקולטה להנדסה חקלאית, הטכניון וד"ר דרור אנג'ל מהמחלקה לציוויליזציות ימיות, אוניברסיטת חיפה. תודות רבות לשניהם על תמיכתם ועל העידוד הרב. אני מודה לפקולטה להנדסה אזרחית וסביבתית במוסד הטכניון על התמיכה הכספית הנדיבה.

הדינאמיקה העונתית של חומר אורגני מומס כרומופורי באגם כנרת: חקירה של שינויים ברכיבים פלורוסנטים ביחס ליצרנות מיקרוביאלית ופיטופלנקטונית.

חיבור על מחקר

לשם מילוי חלקי של הדרישות לקבלת התואר
מגיסטר למדעים במדעי ההנדסה חקלאית

יהונתן ליברזון

הוגש לסנט הטכניון - מכון טכנולוגי לישראל
שבט תשע"ב חיפה ינואר 2011